C 254

Babcock & Wilcox
a McDermott company

Research and Development Division
Lynchburg Research Center
Lynchburg, Virginia 24505

To

E.J. DOMALESKI, NPD

From

G.O. HAYNER, NUCLEAR MATERIALS, LRC
T.J. ZEH, NUCLEAR MATERIALS, LRC

Cust.

TOLEDO EDISON CO.

File No. or Ref.

RDD:85:5104-02:03

Subj.

EXAMINATION OF CRDM LEAFSPRING AND FOREIGN DEBRIS SAMPLES REMOVED FROM DAVIS BESSE-1

Date

MAY 13, 1985

This letter to cover one customer and one subject only.

SUMMARY

An examination was performed at the Lynchburg Research Center (LRC) on ten control rod drive mechanism (CRDM) leafspring samples and three pieces of debris material removed from the Davis Besse-1 nuclear plant. The leafspring specimens included the following: 1) five unbroken leafsprings (with nuts) removed from core locations H-12, L-6, E-5, O-5 and H-6; 2) two broken leafsprings (with nuts) removed from core locations E-3 and M-5; 3) another broken leafspring (with nut) removed from the CRDM test facility at the Alliance Research Center (ARC); 4) a third broken leafspring (with nut) originally sent to the LRC in 1981 from core location C-7; 5) and 4 new leafspring removed from the B&W Parts Center. The three small pieces of debris had been removed from CRDM location E-3 which contained one of the broken leafsprings. An examination of these parts performed on a priority basis has revealed the following summary results: 1) Failure of the leafsprings was probably caused by excessive mechanically induced bending stress which may have been assisted by an embrittlement mechanism; 2) the inservice spring material has a wide range of notch sensitivity and can offer a low margin of safety at a range of loading rates; 3) all springs conform to the bulk chemistry specification range for 17-7 pH stainless steel; 4) the springs have a hardness range from 38 to 47 RC; 5) all of the springs which have failed in service to date are from one material heat; 6) springs evaluated from a second material heat show different metallographic and fracture characteristics when compared to springs fabricated from the first heat; 7) the foreign debris material is apparently fragments from one or more 1/4-inch x 20 threads per inch (1/4 x 20) martensitic steel Allen head set screws.

DISTRIBUTION

LRC

P.S. Ayres
H.H. Davis
T.C. Engelder
G.O. Hayner (10)
Library (2)
T.J. Zeh
S.C. Inman
W.A. Pavinich

ARC

CIS Library (3)
W. Markert
L.W. Sarver
R.K. Bhada

NPD

Library (2)
J.L. Smith
A.L. Lowe

1. INTRODUCTION

Thirteen leafsprings and three pieces of debris material were received at the Lynchburg Research Center (LRC) during March 28 thru April 30, 1985. These are fully identified as follows:

1. Part Number 706362-1101 (subsequently referred to as a leadscrew nut) with an unbroken leafspring (part number 705031-1104) attached to it by two rivets were removed from Davis Besse 1 core location H-12 and are shown in Figure 1. This unbroken leafspring is subsequently referred to as DB-1.

2. A leadscrew nut with a portion of a broken leafspring attached to it was removed from core location E-3. The portion of the leafspring originally attached to the nut is shown in Figure 2. A large part of the remainder of the leafspring was recovered from another location in the CRDM, and is shown here in Figure 3. These two portions of this broken leafspring are labeled DB-5 for this examination.

3. A leadscrew nut with a portion of a broken leafspring attached to it was removed from the CRDM test facility at ARC. These parts are shown in Figure 4. This broken spring is labeled DB-6.

4. Four new, unbroken leafsprings were removed from the B&W Parts Center for comparison to these others. One of these springs is shown in Figure 5, and is called DB-7. The other three springs were labeled DB-14, 15 and 16.

5. A leadscrew nut with an unbroken spring removed from core location L-6 is labeled DB-9.

6. A leadscrew nut with a spring partially broken through one segment of a rivet area, removed from core location M-5 at Davis-Besse. This broken spring is labeled DB-10.

7. Three leadscrew nuts with unbroken springs removed from core locations E-5, O-5 and H-6 are labeled DB-11, DB-12 and DB-13, respectively.

8. Three pieces of debris (foreign material) were removed from the CRDM which contained the broken spring DB-5. These are shown in Figure 6, and are labeled DB-2, DB-3 and DB-4.

In addition to these parts, the broken leafspring received in 1981 (from Davis-Besse) was retrieved from storage at the LRC. Some macro-photography and scanning electron microscopy had been performed on this piece in 1981 to characterize the fracture type, and is reported in Reference 1. Additional analyses were performed during this examination to more fully characterize the failure mode and for comparison with the current springs being investigated. This leafspring is now labeled as DB-8 in this report.

A complete listing of all the measurements and examinations performed on the leafsprings and debris specimens is given in Table 1. The key results obtained from the examination are described in this report, although most of the photographs are omitted for brevity. All of these are available for inspection at the LRC.

Table 1

Leafspring and Debris Examination Summary

Heat -	300130	N/A	N/A	N/A	300130	300130		300130	610073	300130	610073	610073	300130	230232	230232	230232
DB Core Location -	H-12	N/A	N/A	N/A	E-3	N/A	N/A	C-7	L-6	M-5	E-5	O-5	H-6	N/A	N/A	N/A
Description -	Intact Spring	Debris	Debris	Debris	1985 Broken Spring	ARC Broken Spring	Parts Center Spring	1981 Broken Spring	Intact Spring	Broken Spring	Intact Spring	Intact Spring	Intact Spring	Parts Center Spring	Parts Center Spring	Parts Center Spring
B&W ID -	DB-1	DB-2	DB-3	DB-4	DB-5	DB-6	DB-7	DB-8	DB-9	DB-10	DB-11	DB-12	DB-13	DB-14	DB-15	DB-16
Examinations Performed																
Macrophotography	X	X	X	X	X	X	X	-	X	X	X	X	X	-	-	-
Dye Penetrant Exam	X	N/A	N/A	N/A	-	X	-	-	X	X	-	-	-	-	-	-
Rockwell-C Hardness	X	N/A	N/A	N/A	X	X	X	X	X	X	X	X	X	-	-	-
Microhardness	X	X	X	X	X	X	X	X	X	X	-	-	-	-	-	-
SEM - Service Fracture																
- Uncleaned	N/A	-	X	-	X	X	N/A	-	N/A	X	N/A	N/A	N/A	N/A	N/A	N/A
- Cleaned	N/A	-	-	-	X	X	N/A	-	N/A	-	N/A	N/A	N/A	N/A	N/A	N/A
SEM - Lab Fracture	X	N/A	N/A	N/A	X	X	X	X	X	X	-	-	-	-	-	-
Metallography	X	X	X	X	X	X	X	X	X	X	-	-	-	X	-	-
SEM - Etched																
Metallographic Samples	X	X	X	X	X	X	X	X	X	X	-	-	-	-	-	-
Bulk Chemistry																
- Emission Spectroscopy	X	-	-	-	X	X	X	X	X	-	-	-	-	-	-	-
- Atomic Absorption	X	-	-	-	X	-	X	X	-	-	-	-	-	-	-	-
- LECO Carbon	X	-	-	-	X	-	X	X	-	-	-	-	-	-	-	-
Bulk Chemistry (Confirmation - Performed by Ledoux & Co.)	X	-	-	-	X	-	X	-	X	X	-	-	-	-	-	-
Three Point Notched Bend Test At																
Elevated Temperature	-	-	-	-	-	-	-	-	-	X	X	X	X	X	X	X
SEM - Notched Bend Test Fractures	-	-	-	-	-	-	-	-	-	X	X	X	X	X	X	X
Microprobe	-	-	-	-	-	-	-	-	-	X	-	-	-	-	-	-

N/A - Not Applicable

2.1 Macrophotography

All of the intact and broken springs received (except DB-14, 15 and 16) were photographed in detail using a macrocamera. The debris samples were also photographed in a similar manner. Several of the more general photographs were used in the introduction to define the specimens received. In this section photographic information will be presented in more detail for broken springs DB-5, DB-6 and DB-10. Similar information will also be presented for the debris samples. Macrophotography on intact springs DB-1, DB-7, DB-9, DB-11, DB-12 and DB-13 are not given in this section, however, these results are on file for future inspection. The broken spring examined at the LRC in 1981 was not photographed during this examination. Photographic results performed previously are given in Reference 1.

2.1.1 Debris Samples DB-2, DB-3 and DB-4

A photograph of the debris samples from the opposite side from that shown in Figure 6 is given in Figure 7. A part of what appears to be a hexagon shaped slot is shown in the debris sample on the left (labeled DB-3). An end view of sample DB-3 is shown in Figure 8. A detailed photograph showing the bottom of the slot in specimen DB-3 is shown in Figure 9. The extrapolated diameter of specimen DB-3 (based on Figure 8) is 1/4-inch. The thread size is 20 threads/inch (based on Figure 6). A thread pitch gage was also used which confirmed the thread pitch. Therefore, based on the photographic examination, the debris samples are apparently from one or more 1/4-20 Allen head set screws.

2.1.2 Broken Spring Specimen DB-5

The top and the bottom (side closest to the leadscrew nut) of the as-received DB-5 detached broken spring specimen are shown in Figures 10 and 11, respectively. This specimen appeared to be at least partially magnetic. The larger fracture surface (on the right) was previously labeled A (Figure 3).

The fracture surface on the opposite end was labeled B. As indicated, the fractures occurred at the fillet end (A) and beyond the second rivet hole (B). Fracture surface A is shown in Figure 12. The lighter area near the top of the photograph is an impact zone which can be seen with difficulty in Figure 11. The top surface of the fracture is actually the bottom of the spring. A more detailed photograph of the center of fracture surface A is shown in Figure 13. The impact zone is at the upper left side of the photograph. The entire fracture surface and impact zone is covered with surface deposits. The impact zone on the bottom at a location near the center of the fracture infers that the impact occurred after the formation of fracture surface A.

Fracture surface B is shown in the as-received condition in Figure 14. As indicated by the location of the pin, the bottom edge of the fracture surface corresponds to the bottom edge of the spring. This fracture surface has several impact zones one of which can be easily seen at the lower left side of Figure 14. Others which cannot be easily seen are located at the lower edge of the fracture surface on the left side (adjacent to the impact zone mentioned above) and an area on the right edge of the photograph. These areas will be seen more easily in subsequent photographs. A zone of secondary cracking was also seen on the right side near the top of the fracture surface.

The portion of the DB-5 spring which was attached to the leadscrew nut when received at the LRC was inadvertantly not photographed in the as-received condition. This portion of the spring was removed from the leadscrew nut by drilling out both rivet holes. One of the ears containing a rivet hole was used as a notched laboratory fracture specimen. This portion of DB-5 is shown following removal from the nut and fracture of the ear in Figures 15 and 16. Figures 15 and 16 show the top side and bottom sides, respectively. A photograph of the in situ fracture surface is shown in Figure 17. The fillet areas are shown at each end of the photograph.

CRDM part number 706329-1145 (subsequently called the torque tube cap) from core location E-3 (DB-5 location) was also shipped to the LRC for photographic

examination. This part is seen in a side view in Figure 18. A deformed or chipped area was noted at the smaller diameter (non-threaded) end as seen in Figure 19. More detailed views of the deformed area are shown in Figure 20. The deformation apparently occurred at different times. The dark area was smooth and discolored indicating that it had not formed recently. The lighter surface abrasions were recently formed and correspond closely to the width of the spring tip. Apparently the spring tip contacted the torque tube cap when the spring was in the retracted position near the ID surface of the cap. Because of the contact force and the spring taper, the contact surface extended toward the center of the cross section. Apparently the fillet end fracture of DB-5 probably broke from this contact at the outer edge of the contact area.

2.1.3 ARC Broken Spring, DB-6

As indicated previously in Figure 4, this spring broke at the location of the second rivet hole. Macrophotography of interest for this spring were taken during SEM examination and will be presented in Section 2.4.

2.1.4 Broken Spring DB-10

Spring DB-10 was determined to be fractured on one side of the second rivet hole (one of two that holds the pin in place) closest to the end of the spring. This fractured area is seen looking from the top and the bottom of the spring in Figures 21 and 22, respectively. The fracture surfaces are slightly separated and the lower ligament near the outer edge of the spring is protruding slightly. These observations indicate that the rivet was exerting stress on the spring which was subsequently relieved by the crack. The crack occurs at an inclined angle near one side of the rivet hole. The crack seen in spring DB-8 also occurs at an inclined angle near the back of the first rivet. The location and orientation of the cracks is undoubtedly related to the stress distribution around the rivet hole.

The end of spring DB-10 did not show any deformed areas indicating side or end impact loading. However, the oxide layer is scratched on the bottom. One way this could occur is for the spring retracting tool to contact the tapered area of the spring end while the pin was not centered in the slot and temporarily stuck in position. The rounded surface of the retracting tool could scratch the oxide. A series of four photographs are shown in Figure 23 which view the end of the spring from 4 orientations.

The crack noted previously, was opened by impacting the spring on the side containing the crack. This was performed by holding the bottom end of the spring in a vice and impacting on the side near the top. A bottom view of the fracture profile is seen in Figure 24. A macrophotograph of the in situ fracture surface is shown in Figure 25. This fracture probably initiated on the bottom surface and propagated upward and may have been caused by a bending stress applied preferentially to one side of the rivet.

2.2 Dye Penetrant Examination

A fluorescent dye penetrant examination was performed according to ASNTC-1A Codes on the front and back of leafsprings DB-1, DB-6, DB-9 and DB-10. No indications of cracking were seen on any spring. However, pitting was seen during the inspection of DB-1. The pitting which was seen on the top (surface viewed in Figure 1) was less severe and less extensive than the pitting found on the bottom surface.

2.3 Hardness Testing

Rockwell C hardness tests were performed at multiple locations on all spring samples. The tests were performed in accordance with ASTM procedure E18 using a diamond penetrator. The Wilson tester was verified daily before testing and had a maximum repeatability of 0.8 and an error of 0.8. The tests were performed on the surface of the spring. The surface was cleaned but no attempt was made to grind or prepare the spring surface. The mean and standard deviation for the results of each spring was calculated. A summary

of all these measurements are given in Table 2. The large variation in the mean hardness in the 300130 heat may have been attributed to the slightly pitted surface of these springs. A statistical test (t-test) was performed on the results from the two heats of spring material to determine if there was a difference between the mean hardness values. The test results showed that the means were not equivalent and that the 610073 heat was harder than the 300130 heat. In addition, a Vickers diamond pyramid microhardness measurement was performed at three locations on springs DB-1, DB-5, DB-6, DB-7, DB-8, DB-9 and DB-10, as well as one location on each of the three debris specimens. The testing was performed in accordance to ASTM procedure E-92. These values were then averaged (for each specimen) and converted to the Rockwell C equivalent value using the ASTM E-140 conversion tables.

Table 2

Summary of Hardness Inspection Results

Hardness Measurement	Spring Number - B&W ID/Heat									
	DB-1	DB-5	DB-6	DB-7	DB-8	DB-9	DB-10	DB-11	DB-12	DB-13
	300130	300130	300130	300130	300130	610073	300130	610073	610073	300130
Rockwell C	44.5	40.6	45.5	41.2	38.5	46.9	39.9	46.9	45.6	44.7
Standard Deviation	0.9	2.3	1.2	0.2	0.5	0.7	1.4	0.7	0.7	0.5
Vickers Micro-hardness	441	381	411	390	401	454	367	-	-	-
Standard Deviation	1.73	14.8	12.5	0	14.5	7.5	7.5	-	-	-
Vickers Conversion to Rockwell C	44.5	38.8	41.8	40	40.9	45.7	37.3	-	-	-

	B&W Samples - B&W ID		
	DB-2	DB-3	DB-4
Rockwell C	- -	-	
Standard Deviation	- -	-	
Vickers Micro-hardness	495	518	503
Standard Deviation	- -	-	
Vickers Conversion to Rockwell C	48.8	50.3	49.2

Table 2

2.4 Service and Laboratory Fracture Examination

A portion of springs DB-1, DB-5, DB-6, DB-7, DB-8 and DB-9 were purposely fractured in the laboratory by filing a sharp notch across an area of each spring and then impacting it with a hammer. In each case, fracture occurred with a low force hammer blow, and without any apparent bending or ductility. This was confirmed in the Scanning Electron Microscope* examination of the fracture surfaces. Except for DB-7 and DB-9, all of the fractures consisted of a combination of intergranular and quasi-cleavage features, with small areas of ductile rupture. In the case of DB-7, and DB-9 the fracture was transgranular and contained areas of ductile rupture and quasi-cleavage features.

The laboratory tests performed above were performed because one of the potential causes of failure being investigated was a bending load which may have been applied as an impact. In order to quantify these laboratory tests a notched three point bend test in 200°F water was performed on specimens removed from spring samples DB-10, 11, 12, 13, 14, 15 and 16. Specimens 15 and 16 were not notched. The specimen configuration and test setup are shown in Figure 26. Test specimen dimensions given in Figure 26 are nominal. The actual dimensions were measured and used to calculate maximum K_I values given in Table 3. The testing was performed in 200°F water purged with Argon because rising load test data on Inconel X750 has shown that air fracture and fracture in warm water can produce entirely different fracture morphologies and failure times for the same material. For the Inconel X750 material, the fractures which occur in warm water tend to be more intergranular. Therefore, the spring specimens were tested in warm water because the actual fractures occurred in low temperature water due to the known fracture morphology change for the Inconel X750 material. The bend testing was originally to be performed at fast (0.5-inch/sec) and slow (0.05 inches/sec.) loading rates in

*The Etec Scanning electron Microscope records pertinent data on the photographs as illustrated below:

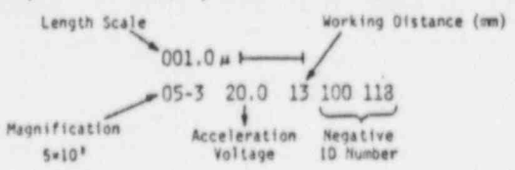

Table 3

Summary of Three Point Bend Test Results
Performed in 200°F Water

Spring ID	Heat	in/sec	Max. Load, lG	Fracture Morphology	Estimated $K_{I(max)}$
DB-10	300130	0.5	68.3	Intergranular	45.6
DB-11	610073	8.3×10^{-4}	31.8	Transgranular	21.2
DB-12	610073	0.5	85.5	Transgranular	53.9
DB-13[1]	300130	3	-	Intergranular	-
DB-14	230232	0.5	27	Ductile Rupture	50.3
DB-15	230232	0.5	90	No Fracture	-
DB-16	230232	0.5	70	No Fracture	-

[1]Machine Malfunction

each material heat to be tested (i.e., heats 300130, 610073 and 230232). However, due to both testing machine malfunction and operator error, the specimen machined from spring DB-13 (heat 300130) was tested at approximately 3 inches/sec load rates and the specimen removed from DB-11 was tested at 0.05 inches/min. The results obtained from these tests are given in Table 3. The fractures obtained from these tests performed on the specimens from heat 300130 were quite similar to the fracture morphologies for DB-5, 6, 8 and 10 service failures. Typical SEM photographs obtained which compose the service and laboratory testing fracture morphologies are shown in Figure 27. Fracture morphologies obtained from specimens machined from DB-11 and 12 (heat 610073) were entirely dissimilar. Representative photographs taken on these fracture surfaces are shown in Figures 28 and 29. Both of the fractures occurred at an angle of approximately 45° to the top of the spring surface. However, the fractures from the 300130 were nearly normal to the top spring surface. The fracture surfaces obtained from DB-11 and 12 were entirely transgranular and contained various combinations of quasi-cleavage and ductile rupture. The fracture of the 230232 heat which had not been in service was entirely ductile rupture. Representative photographs are shown in Figures 30 and 31. The unnotched specimens did not fracture during testing.

An SEM examination was performed on fractured ends A and B (Figure 3) of DB-5 prior to and following cleaning in inhibited HCl solution (6N). A similar examination was also performed on the DB-6, and DB-10 fracture surfaces. These results indicated that the fractures occurred intergranularly and that fracture initiation was from the bottom surface in all cases. Similar results had also been obtained during the examination of the DB-8 fracture surface in 1981 (Reference 1).

After cleaning, fracture surfaces A and B from DB-5 were examined in detail using the SEM. The fracture surfaces were almost entirely intergranular. Several impact zones were seen while performing the examination. Figure 32 gives an SEM photograph of the DB-5 location A fracture surface. The impact zones are labeled as A and B. A detail of area A is given in Figure 33. The cracks that can be seen normal to the fracture surface were apparently caused

by the impact which deformed the fracture surfaces above the lower crack (darker gray area). The fact that localized deformation of this type would cause cracking normal to the primary fracture surface is an indication of the brittleness of the material. Area B, which is a much smaller and more localized area is shown in Figure 34. Areas A and B impact zones may have been formed at the time that the small end of the spring.

An SEM photograph of the DB-5 location B fracture (small end fracture) is shown in Figure 35. This fracture is at the base of the tapered area (ski jump) at the end of the spring. The largest impact zone (Area A) is illustrated in Figure 36. The large normal crack network observed in Figures 35 and 36 was apparently caused by impact to the end of the spring and along the lower edge in this same area. A second impact zone was also seen at location B. These impacts probably occurred after the fillet end of DB-5 (location A) had fractured. The resulting loose piece could then have been damaged in the CRDM.

An SEM photograph of the DB-6 fracture surfaces A and B is given in Figure 37. The rivet, pin assembly and spring fracture surface on both sides of the rivet are shown. The A half of the fracture is slightly inclined from perpendicular to the longitudinal axis of the spring. The B half is close to perpendicular (normal to the spring axis). One of the fractures in spring DB-8 and the in situ fracture in spring DB-10 were inclined at a greater angle (from perpendicular) than fracture A. The presence of a crack at an angle associated with the rivet hole (as discussed above) implies that the rivet is exerting a considerable stress on the rivet hole. This stress is being exerted in all directions around the circumference of the hole. Another indication of this stress was mentioned previously in Section 2.1 for spring DB-10. The magnitude of the axial stress vector across the rivet hole apparently causes the maximum stress intensity coutour to deviate from an angle normal to the axis of the spring. A larger amount of rivet hole stress would cause a larger angle of deviation. Also, the fractures which are not normal to rivet holes are apparently those which occurred first, i.e., before the stress was relieved in the rivet hole area by the initial fracture.

Therefore, by this argument, fracture A occurred prior to fracture B. Fracture A clearly initiated at the bottom and was caused by a bending stress. This is also indicated by the upward deformation noted on the bottom of the rivet top. Details of fractures A and B are shown in Figure 38. Both fractures were predominately intergranular.

The fracture surface generated by opening the DB-10 crack noted previously was examined using the SEM. An SEM photograph of the in situ and lab fracture surfaces with the rivet hole between is shown in Figure 39. The side labeled C is the in situ service fracture. A more detailed photograph of the in situ fracture is given in Figure 40. The bottom surface of the spring is downward in this figure. The fracture surface is primarily intergranular with crack propagation from bottom to top. An energy dispersive X-ray (EDX) spectrum of the fracture surface shown in Figure 40 is given in Figure 41. This spectrum indicates that the major elements present with atomic numbers $\geq$ Na are Cr, Fe and Ni. Lesser amounts of Al and Si were also detected with trace amounts of Ca and Ti. Si and Ca are present in small amounts in the primary water. All other elements noted are present in the spring composition.

An SEM photograph of area D (Figure 39) is given in Figure 42. A small cracked area (labeled r) was seen that intercepted the rivet hole. The top of the spring is in the lower right of the photograph. It was determined from more detailed examination that the small crack under cuts a portion of the rivet hole/fracture surface interface and also intercepts the main fracture surface and the top surface of the spring. This crack apparently initiated on the top surface of the spring after the main fracture had occurred and is probably unrelated to the main fracture. A more detailed photograph of area r is shown in Figure 43. An EDX spectrum of the rivet hole surface seen in Figure 43 is shown in Figure 44. The elements detected included Al, Si, Cr, Fe and Ni. Elements (such as S or Cl) from compounds which could contribute to a corrosive environment in the crevice area were not detected.

2.5 Metallographic Examination

A metallographic exmination was performed on all spring samples except DB-11, 12, 13, 15 and 16. The debris samples were also examined metallographically. All specimens were decontaminated in passivated HCl to remove surface contamination and mounted in thermosetting epoxy in a standard mounting press. The specimens were then wet ground with 180, 240, 400 and 600 grit silicon carbide papers. Following grinding, the samples were mechanically polished with 1.0, 0.1 and 0.05 micron alumina polishing compound. The spring specimens were etched electrolytically in 10% ammonium persulfate at 3 volts potential for 30 seconds. The debris samples were etched in a 5% nital solution for 2 seconds.

Figure 45 shows the typical microstructure observed for springs DB-1, 5, 6, 8 and 10 from heat 300130 and DB-14 from heat 230232. This microstructure is characteristic of the TH-1050 heat treatment for 17-7 pH stainless steel.(2) The upper photomicrographs are optical micrographs of DB-5 after etching. The lower photomicrographs are SEM secondary electron images (SE) of the metallographically prepared surface of spring DB-5 after etching. The optical micrographs show stringers and globules of ferrite in a martensite matrix. The grain boundaries are partial carbide networks, probably Cr23C6, which are typical of this heat treatment. The chromium carbides form during the austenite conditioning treatment, first at the ferrite - austenite interface and then, if the carbon is on the high side, at austenite grain boundaries.(3) The ditches in the SEM micrograph also show this and result from the etchant selectively attacking the Cr depleted zones adjacent to the grain boundaries.

The heat 610073 microstructure (spring DB-9) showed a distorted microstructure which would be characteristic of cold worked condition A sheet stock being used as the starting material rather than annealed sheet (condition A). If cold worked sheet stock was used as the starting material, the martensite transformation would take place during cold work (prior to heat treatment). Subsequent heat treatment at 1400°F and 1050°F for 90 min. would cause recrystallization and overaging. The heat treatment received by the 610073

heat material is not certain. The furnace records show the material was heat treated at the same temperatures as the 300130 heat, but the chart speed was not recorded on the furnace charts. Hence, the holding times at these temperatures are uncertain. Figure 46 shows optical and SEM photomicrographs of spring DB-9 from the 610073 heat. The grain structure of the 610073 heat is distorted, typical of a cold worked microstructure. Figure 47 and 48 show comparisons of the microstructures from the two heats. The upper photomicrograph in Figure 47 is representative of the 300130 (TH-1050) heat and the bottom that of the 610073 heat. Figure 48 shows the optical micrographs of the spring as viewed from the top, side and end of the spring. It is apparent that in both cases the axis of the spring is parallel to the rolling direction of the sheet stock and that the microstructure of the 300130 and 610073 heats are not similar.

The microstructure of the debris samples DB-2, 3 and 4 (Figure 49) was a normal tempered martensitic structure. The EDS system on the SEM was used to qualitatively determine the major chemical constituents of the material. Results showed the alloy was primarily iron with a small amount of silicon. (The EDS system does not detect elements in concentrations under 1 weight percent or elements with an atomic number less than that of sodium). These results indicate that the debris material is probably plain carbon steel. This is consistent with the facts i.e.; the samples were magnetic, a large amount of iron oxide corrosion product was found on the samples during the visual examination, and Allen-Head set screws are fabricated from a plain carbon steel.

2.6 Bulk Chemistry

Bulk Chemistry was determined on samples removed from springs DB-1, DB-5, DB-6, DB-7, DB-8 and DB-9 using emission spectroscopy. A Jerrel-Ash Atom Comp Model 750 direct reading spectrograph was used. Calibration was performed using a set of 6 stainless steel standards according to the Jerrel-Ash recommended procedure. All samples were burned three times and the results were averaged according to normal procedure. All burns were normal except

DB-5, which showed a much shallower burn depression than the other samples or standards. The reason for this apparent response difference is unknown.

The Cr, Ni and Al results were checked using atomic absorption (AA) spectroscopy on dissolved samples of turnings removed from each sample. Carbon was determined by using a LECO carbon analyzer (combustion method). A summary of the chemistry results compared to the 17-7 pH stainless steel chemical composition range specification is given in Table 4. Because of the shallow burn depth noted on sample DB-5, the emission spectroscopy data for this sample should be ignored and is not included in Table 4. The estimated absolute analysis error for each element is also given in Table 4. As a check, samples from DB-1, DB-5, DB-7, DB-9 and DB-10 were sent to Ledoux and Company for Bulk Chemical Analysis. These results are also shown in Table 4. As indicated, all of the spring material meets the 17-7 pH stainless steel bulk chemistry specification range for the elements analyzed.

2.7 Microprobe Examination

A portion of the rivet hole surface and the in situ fracture surface removed from DB-10 was examined using a Cameca electron microprobe at the Massachusetts Institute of Technology. This instrument is equipped with a 3-crystal wavelength dispersive spectrometer. Qualitative wavelength spectra were obtained at several locations in the rivet hole and fracture surface using a 20A square area scan. This examination was performed primarily to verify the EDX results given previously. The microprobe examination detected only elements associated with the 17-7 bulk composition or elements normally seen in primary water including Fe, Cr, Ni, Si, Al, and Ti. Elements (such as S or Cl) from compounds which could contribute to a corrosive environment in the crevice area were not detected.

Table 4

Summary of Bulk Chemistry Results

Results in w/o

Spring Analyzed

Type Test(1)	Element Analyzed		DB-1(3)	DB-5(2)	DB-6	DB-7	DB-8	DB-9	17-7 Bulk Chemistry Range
EM	Si	(0.006)(4)	0.45	-	0.44	<0.23	0.46	0.44	1.00 Max
	MN	(0.12)	0.64	-	0.64	0.74	0.63	0.53	1.00 Max
	P	(0.004)	<0.018	-	<.018	0.019	<0.018	<0.018	0.040 Max
	S	(0.004)	0.007	-	0.010	0.004	0.008	0.011	0.040 Max
	Ni	(0.6)	6.96	-	6.35	5.94	5.83	6.46	6.50-7.75
	Cr	(1.6)	16.6	-	15.9	16.0	15.8	16.4	16.00-18.00
	Mo	(0.3)	0.12	-	0.12	0.34	0.12	0.11	-
	Cu	(0.004)	0.17	-	0.18	0.18	0.20	0.15	-
	Al	NA	>0.026	-	>.030	>0.027	>0.027	>0.03	0.75-1.50
	Co	(0.24)	0.086	-	0.093	0.075	0.10	0.084	-
AA	Ni	(0.24)	7.1	7.5		7.0	7.0		6.50-7.75
	Cr	(1.04)	17.1	16.4		16.9	16.1		16.00-18.00
	Fe	(1.82)	74.2	72.4		71.1	71.1		-
	Al	(0.04)	1.19	1.14		1.04	1.20		0.75-1.50
LC	C	(0.01)	0.086	0.078		0.065	0.076		0.09 Max

(1) Em = Emission Spectroscopy
AA = Atomic Absorption
LC = LECO Carbon Analysis

(2) DB-5 SEM results were not obtained because of abnormal burns

(3) Average of two series of three analyses for EM results

(4) Percent Absolute Error

Ledoux and Company Chemistry Results

Element	Error	DB-1	DB-5	DB-7	DB-9	DB-10
Si	±.05	.47	.48	.32	.48	.48
Mn	±.03	.68	.66	.80	.55	.66
Ni	±.10	7.28	7.22	7.13	7.12	7.20
Cr	±.10	16.85	16.39	16.86	16.68	16.32
Mo	±.02	.10	.09	.25	.09	.09
Cu	±.02	.20	.19	.21	.14	.18
Co	-	<.003	<.003	.005	<.003	<.003
C	±.002	.058	.087	.086	.081	.087
S	±.002	.012	.018	.017	.022	.015
Al		1.60	1.76	1.61	1.81	1.77

Note: Ledoux did not have sufficient material to perform a phosphorous analysis and recheck the Al. They suspect an error in the Al analysis and will recheck the results.

3. DISCUSSION

All of the springs which failed in service (i.e., DB-5, 6, 8 and 10) were from heat 300130 and showed fracture surfaces which were primarily intergranular. Fracture initiation was from the bottom of the springs in all cases. No evidence of any detrimental chemical species was observed during EDS or microprobe examination. The notched 3 point bend test fracture surfaces performed on material removed from DB-10 and 13 (heat 300130) also show mostly intergranular fracture characteristics. The lab fractures and 3 point bend test results also indicate that the material removed from service is quite notch sensitive. This indicates that the primary fracture mode of heat 300130 material in bending with a stress concentrator present is intergranular. It also indicates that the service failure could have resulted from a mechanically induced bending stress. Normally, a primarily intergranular fracture in most materials implies a corrosion induced or hydrogen embrittlement mechanism. Neither of these mechanisms can be eliminated from consideration with the data available. The three point bend testing performed on DB-14, 15, and 16 which had not been in service, shows that 17-7 pH spring material with a similar microstructure to the 300130 material will bend (unnotched) or fracture by ductile rupture in a notched specimen. The possible hydrogen embrittlement mechanism could be proven or disproven by either baking out and testing a notched 3 point bend specimen removed from a 300130 heat spring obtained from service in Davis Besse 1 or testing a specimen from the same heat which had not seen reactor service.

The metallographic results indicate that a grain boundary network is present in all the heat 300130 and 230232 samples examined. The material has nearly equiaxed grain structure, a low carbon martensite matrix, and localized areas of ferrite segregation aligned parallel to the longitudinal axis of the spring. The metallographic results for the DB-9 spring sample (heat 610073) are quite different than the 300130 material. The 610073 material does not contain a pronounced grain boundary network, has non-equiaxed grains and contains greater amounts of laminated ferrite stringers aligned parallel to

longitudinal direction of the spring. However, because the 230232 material fractures transgranularly, other factors such as hydrogen embrittlement may be contributing to the intergranular crack propagation seen in the 300130 material. The grain boundary network in the 300130 material apparently provides a path for mechanically induced crack propagation. The 610073 material fractures transgranularly at about 45° to the top of the spring. The fracture path proceeds by ductile rupture between ferrite stringers and by quasi-cleavage along carbides adjacent to the stringers. This fracture mode may also be caused by an embrittling mechanism.

The visual inspection results indicate that the initial fracture of DB-5 was probably caused by contact with the end of the torque tube cap when the spring was in the retracted position. This is known to be a possible occurrence based on a tolerance study performed at NPD. Based on the probable stress distribution in the spring when this interaction occurred, it is likely that the fillet end fracture occurred first. The fracture at the base of the ski jump apparently occurred by mechanical interaction with the CRDM.

A second type of failure is indicated by scratch marks seen on the bottom of the DB-10 ski jump. This implies interaction with the retracting tool while the spring was resisting the retracting motion. This resistance may have been caused by the pin not being centered in the slot and hanging up on the end or sides of the slot. A small amount of testing at the NPD parts center indicates that the pin can hang up in the slot. If the spring was hung up by the pin, the retractor tool action would tend to break the spring at the rivet closest to the ski jump (second rivet). This is where the break occurred for springs DB-6 and DB-10. This is the most likely mechanism for failure of these springs based on the information available. The situation for DB-8 is less clear because the fracture occurred at the first rivet hole. The most likely mechanism, however, is interaction with the torque tube cap.

Available records indicate that the heat 300130 spring material was heat treated in the TH-1050 condition. This is supported by the spring microstructure results. The TH-1050 condition normally has a hardness range

of Rockwell C 38 to 46. The hardness depends on degree of cold work, grain size, and other factors. The hardness results are in the range from 39 RC for spring DB-8 to 46 RC for spring DB-6. This should be considered to be a normal variation for a single heat treatment. The hardness results for the springs fabricated from heat 610073 material indicate that this material is statistically harder (46-47 RC) than the heat 300130 material. This may be due to the heat treatment or the condition of the original sheet stock material. The heat treat temperatures for the 610073 material correspond with TH-1050 requirements, however, the time at each temperature could not be determined from furnace charts. Also, the metallography results indicate that annealed and cold worked sheet stock was originally used rather than condition A material. The hardness results support the metallographic results.

The bulk chemistry results for the spring material (300130 and 610073 heats) indicate that all samples are within normal 17-7 compositional specifications.

Shallow pitting attack was seen on the bottom of leafspring DB-1 and DB-5. Pitting was not seen on leafspring DB-7 indicating that pitting is not present on new leafsprings prior to service. Information regarding pitting attack on springs DB-6 and DB-8 is not available. The pitting does not appear to be related to the most likely failure mechanism. The locations of the pitting are not in a true crevice area such as the rivet hole. Limited data based on 304 SS/17-7 pH coupled tests performed at Battelle[4] for 1000 hours at 200°F in 2:1 H/O atmosphere with 0.6 w/o boron as boric acid in water indicate that the 17-7 pH is not pitted from either the test solution or contact with 304 SS. Therefore, the origin of the slight pitting cannot be explained with the data available.

The fact that spring failures have occurred only at the Davis Besse 1 plant would initially indicate something unique regarding several variables including: service environment, spring material, spring stress, CRDM operation or maintenance procedures. However, the results of this examination indicates that CRDM operation and maintenance procedures are the most important factors that separate Davis Besse 1 from other B&W plants. There is

no evidence to suggest that the Davis Besse 1 service environment is unique. The four known spring failures have come from one heat of material, however, this heat is used in other B&W plants and meets all 17-7 pH TH-1050 specifications. This is based on hardness, chemical and microstructure examinations performed at the LRC and chemical and mechanical test examinations performed following manufacture. Other spring heats meet the same specifications, therefore, material differences that might separate the failed springs from other springs used in service are absent. The springs and nut assemblies examined were designed normally and therefore should have had nominally the same stress distribution in the fillet and rivet areas as springs used in other plants. None of the evidence indicates that fatigue damage is present and operating information indicates that the springs are rarely left in the retracted position or cycled from the locked to the retracted position. The examination results indicate that the four failed springs probably failed or partially fractured either when the springs were in the retracted position or during the retracting operation. This indicates that these operations have a higher risk of resulting in spring damage and should be avoided, if possible. During the CRDM spring inspection performed at Davis Besse 1, 5 springs were found to be retracted. If it is assumed that springs DB-5 and 8 were also retracted prior to failure, at least 7 springs were left retracted. Inspections have been completed to date at two other plants. One plant had no springs in the retracted position and the second plant had two in this position. The tolerances in the CRDM do not preclude interference between a retracted spring and the torque tube cap. Therefore, the probability of this type of failure is related to the number of springs left retracted during CRDM operation. None of the B&W plants including Davis Besse 1 currently use the manual spring retracting tool. Instead, the alternate uncoupling method is used which acts directly on the torque tube. Manual spring retraction at Davis Besse 1 has not been performed since startup. This implies that the partial fracture seen in DB-10 has been present since startup and that similar fractures may be present (undetected) in other plants.

The information obtained from the analysis of DB-2, 3, and 4 indicates that this foreign material recovered from the CRDM is one or more pieces of 1/4"-20 hardened carbon steel Allen head set screws. This mateiral probably entered the CRDM by dropping out of a tool during CRDM repair operations.

4. CONCLUSIONS

1. The leafsprings examined probably failed in service by mechanically induced overstress. It is suspected that an embrittlement mechanism affected the properties of the springs examined and may have contributed to the inservice failures.

2. The leafspring material removed from service is notch sensitive and will easily fracture at stress risers by mechanical force.

3. All springs examined which were fabricated from heat 300130 material show normal chemical analysis, hardness and microstructural results expected for 17-7 pH stainless steel in the TH-1050 condition. The springs fabricated from heat 610073 material show abnormal TH-1050 microstructure and hardness values.

4. The leafsprings apparently are subjected to a higher risk of failure during manual retraction or by being left in the retracted condition during CRDM operation.

5. The foreign debris material is apparently fragments from one or more 1/4-20 hardened plain carbon steel Allen head set screws.

5. RECOMMENDATIONS

1. All CRDM leafsprings in licensed B&W plants should be examined to verify that:

    a. Each spring is in the engaged position
    b. Each spring is intact

    All retracted springs should be inspected for damage and returned to the engaged position. All failed springs should be examined and replaced.

2. The alternate uncoupling method should continue to be used for CRDM maintenance.

3. The possible hydrogen embrittlement mechanism could be proven or disproven by either baking out and testing a notched 3-point bend specimen removed from a 300130 heat spring obtained from service in Davis Besse 1 or testing a specimen from the same heat which had not seen reactor service. At least one of these alternatives should be pursued.

4. Investigate the fabrication and manufacturing history of heat 610073 material. Attempt to determine the cause of the non-equiaxed grain structure.

5. Perform a further investigation into the cause of the inservice pitting noted.

6. REFERENCES

1. Letter Report LR:81:5386-01:01, "Preliminary Examination of CRDM Leafspring," January 4, 1982.

2. Metals Handbook, 8th Edition, Volume 1, Atlas of Microstructures of Industrial Alloys, American Society for Metals, Metals Park, Ohio, 1972.

3. ARMCO 17-7 PH and PH 15-7 Mo Stainless Steel Sheet and Strip Data Book, Steel Corp., Middletown, Ohio, 1966.

4. W.K. Boyd, et al, "Corrosion in Borated and Deionized Water at Temperatures up to 500°F," BMI-1047, Battelle Memorial Institute, October 14, 1955.

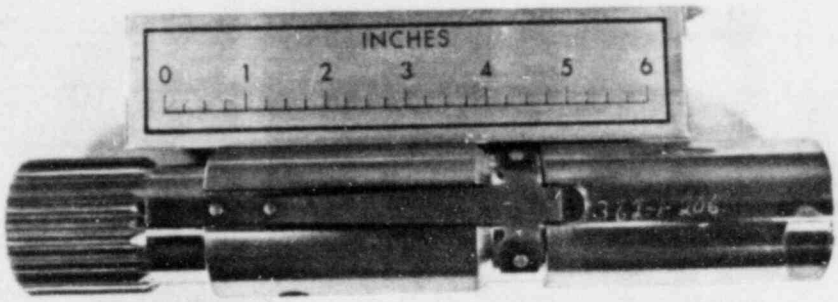

0.4X

F85-1
Figure 1 - Leadscrew Nut and Intact Leafspring DB-1 Attached

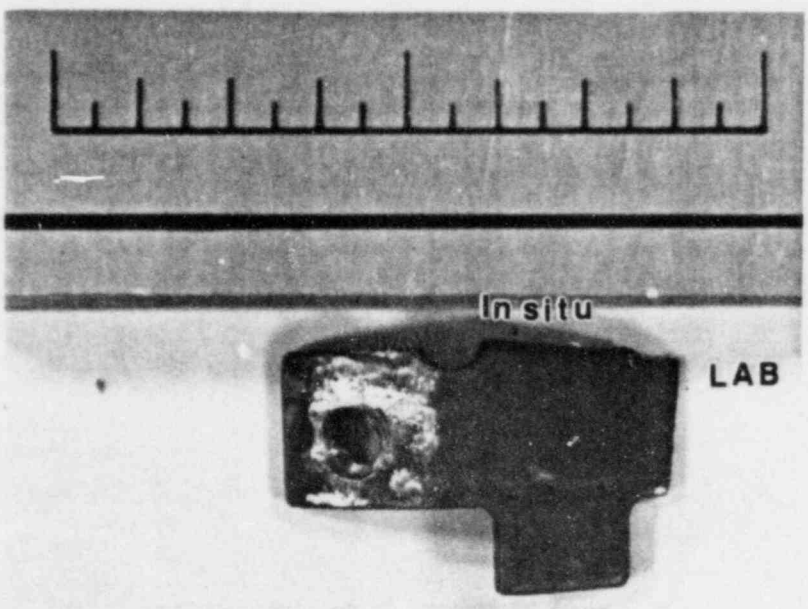

1.8X

F85-41
Figure 2 - Portion of Leafspring Attached to DB-5 After Ear Was Removed During Laboratory Fracture

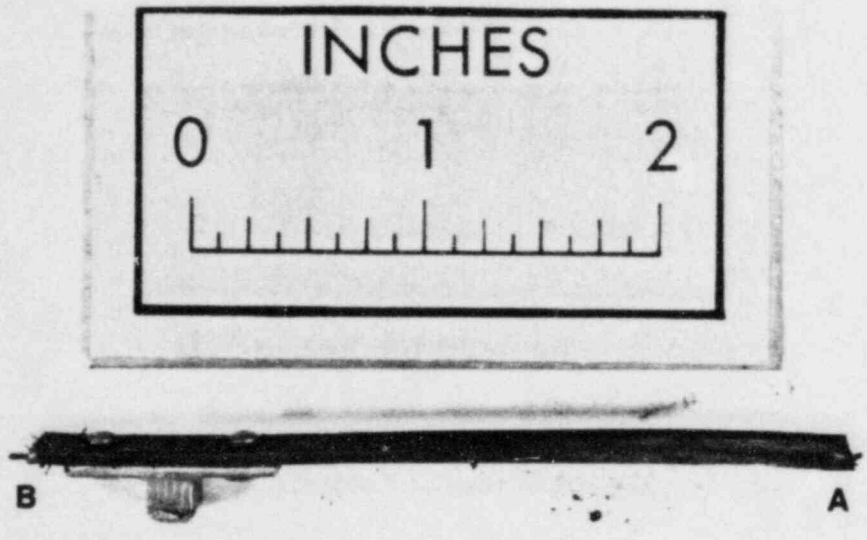

1.2X

F85-19

Figure 3 - Remainder of DB-5 Leafspring. The end (A) on the right side of the photo is the mating surface with the leafspring portion shown in Figure 2. The opposite end fracture (B) mates with a small piece not recovered.

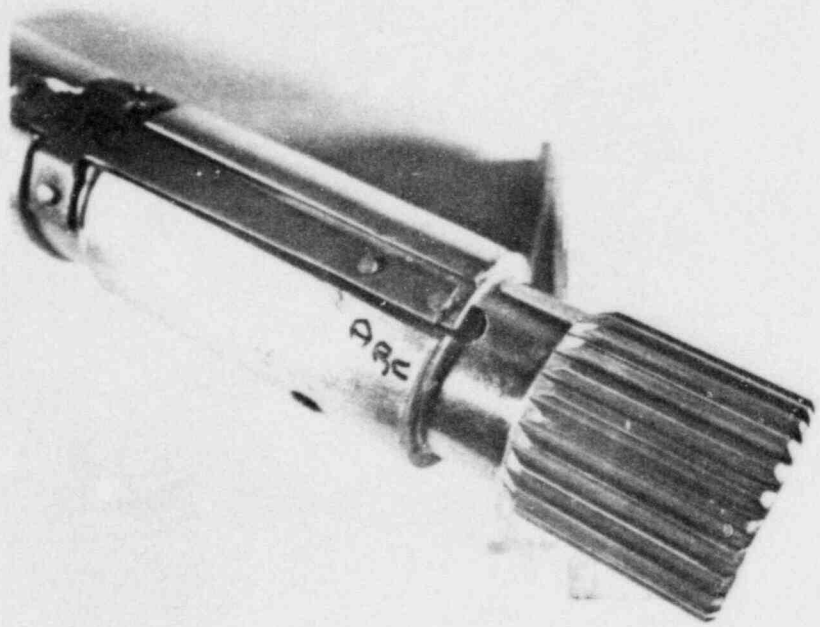

Figure 4 - Leadscrew Nut and Portion of Leafspring DB-6 Attached. Leafspring fracture is adjacent to second rivet near center of photo.

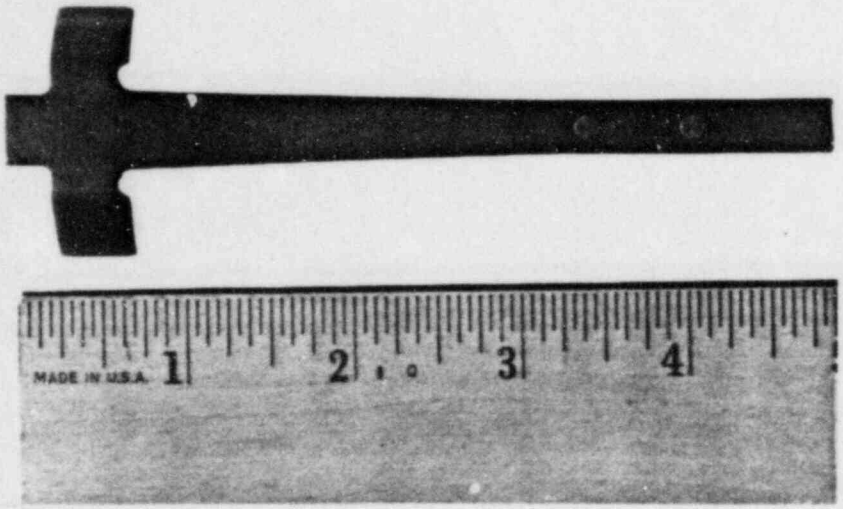

0.8X

M85-158
Figure 5 - New Unbroken Leafspring Removed From the B&W Part Center

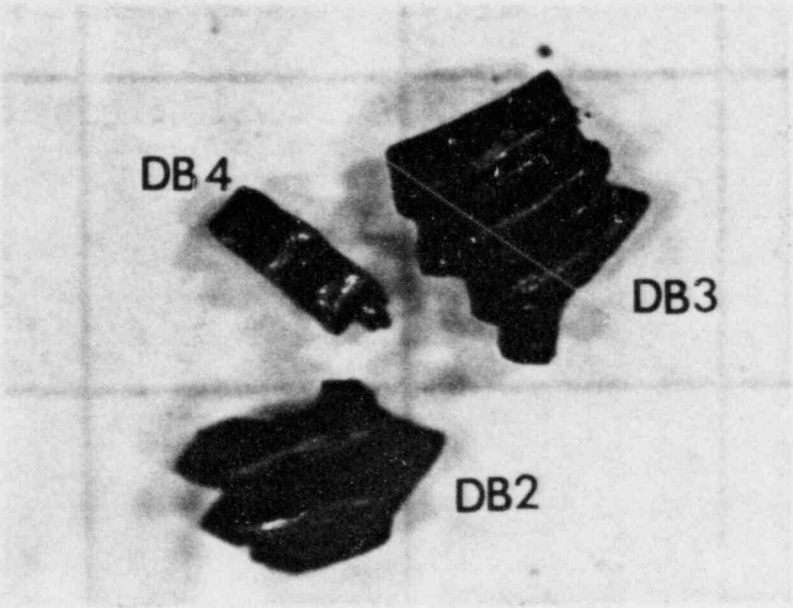

Figure 6 - Debris Particles DB-2, DB-3 and DB-4
Background grid is 1/4"square 1.6X

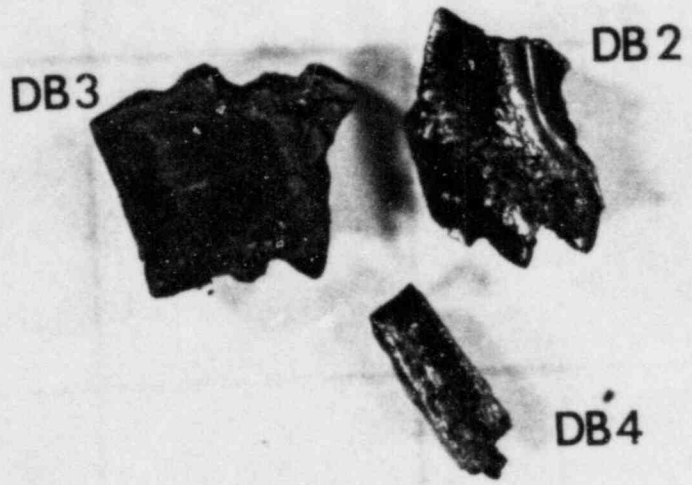

1.6X

Figure 7 - Photomacrographs of the Debris Particles DB-2, DB-3 and DB-4 Showing Hex Shaped Surface.

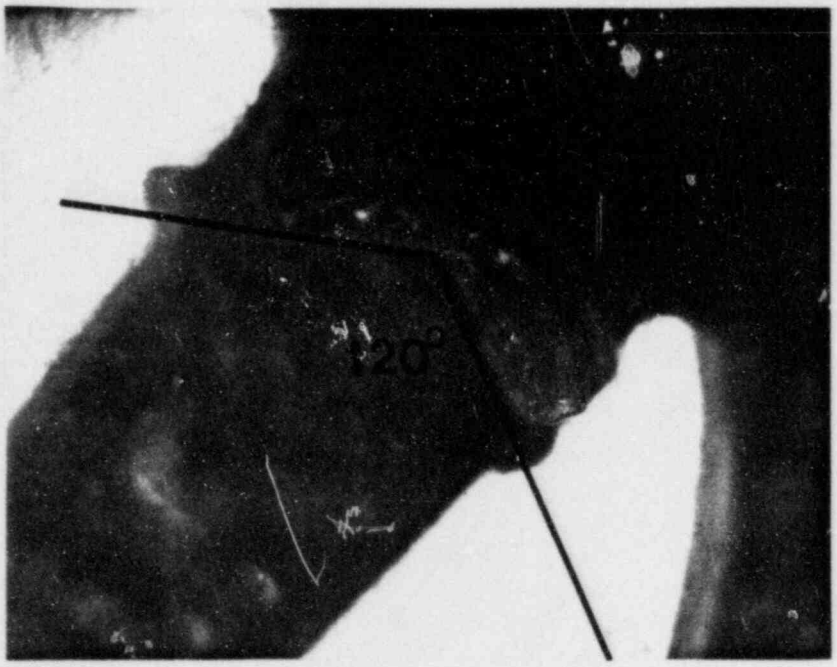

15X

F85-17

Figure 8 - Photomacrograph showing the 120 Degree Angle on the Hex Surface of DB-3.

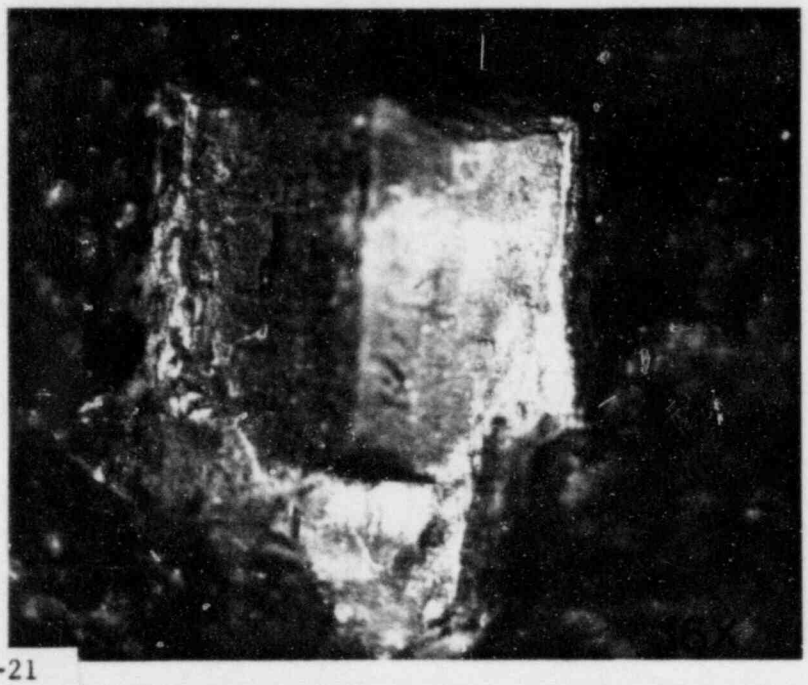

F85-21

Figure 9 - Photomacrograph Showing the Bottom Particle DB-3.

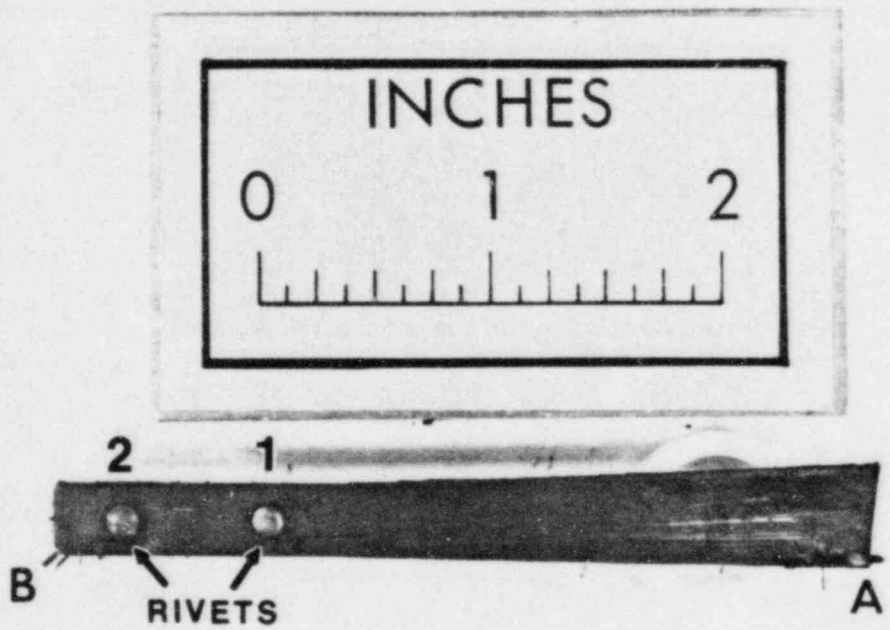

Figure 10 - Photomicrograph of the Top Surface of Spring DB-5. 1.2X

F85-20

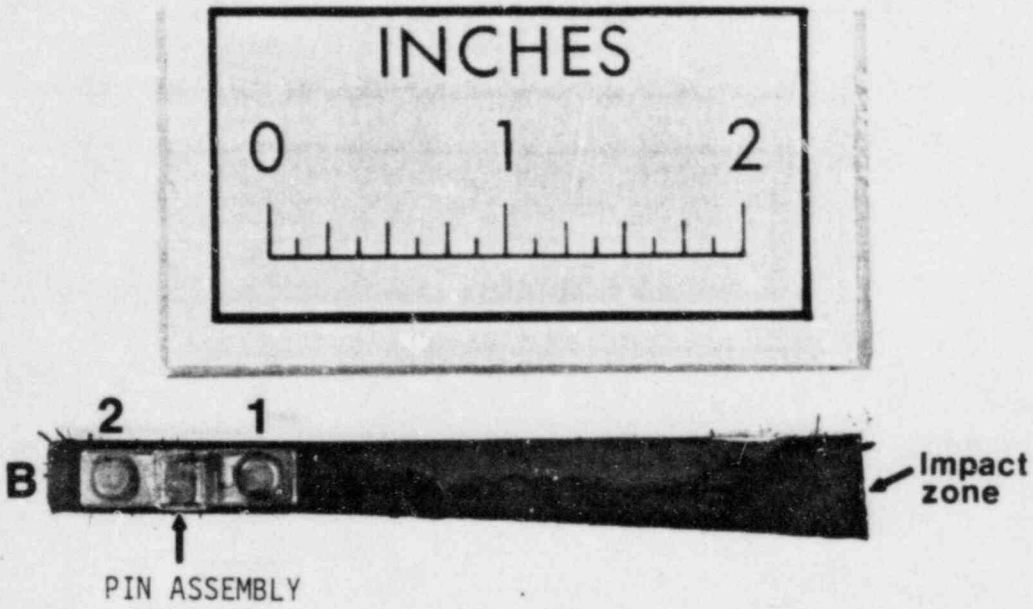

F85-18

Figure 11 - Photomicrograph of the Bottom Surface of Spring DB-5. 1.2X

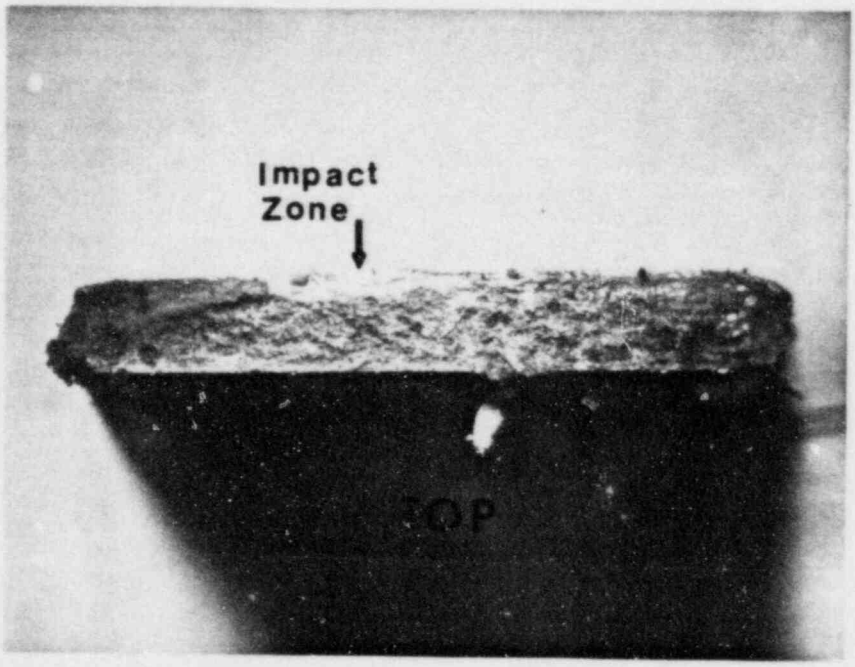

Figure 12 - Fractograph of the Large Fracture, End "A", of Spring DB-5. 8X.

F85-29

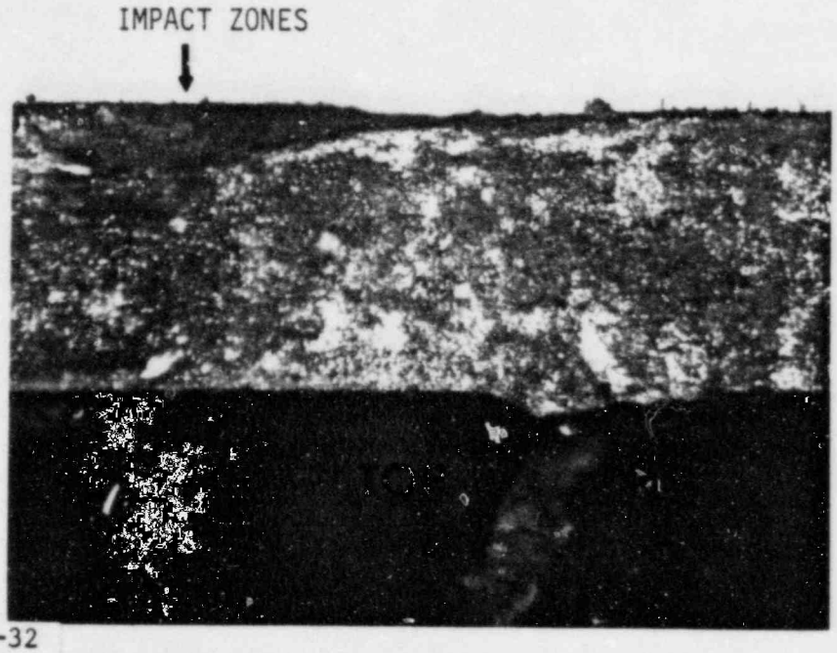

F85-32

Figure 13 - Fractograph of the Center of the Figure 12. 23X.

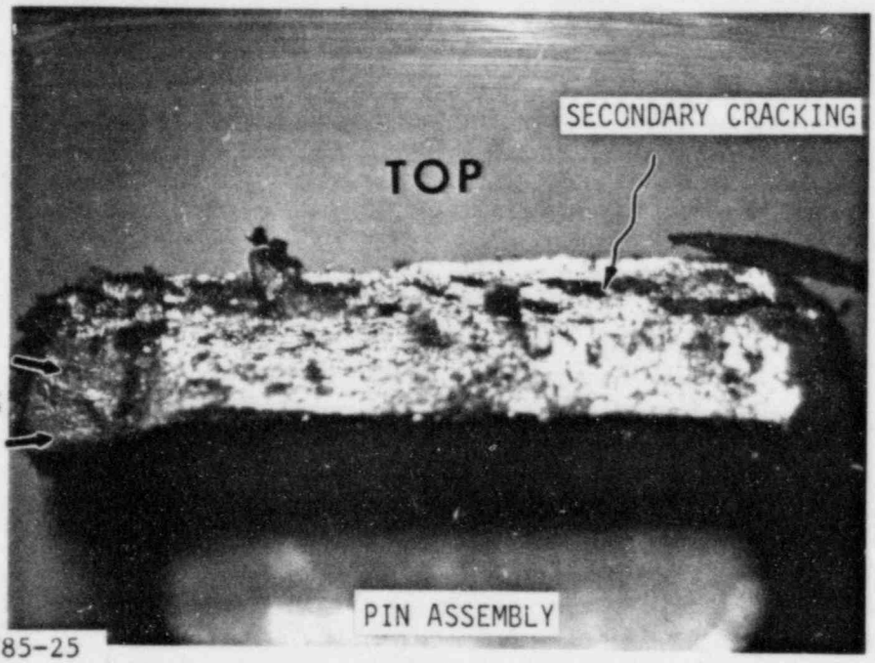

F85-25

Figure 14 - Fractograph of the Small Fracture Surface of Spring DB-5, End "B", in the As-Received Condition Showing Impact Zones. 8X.

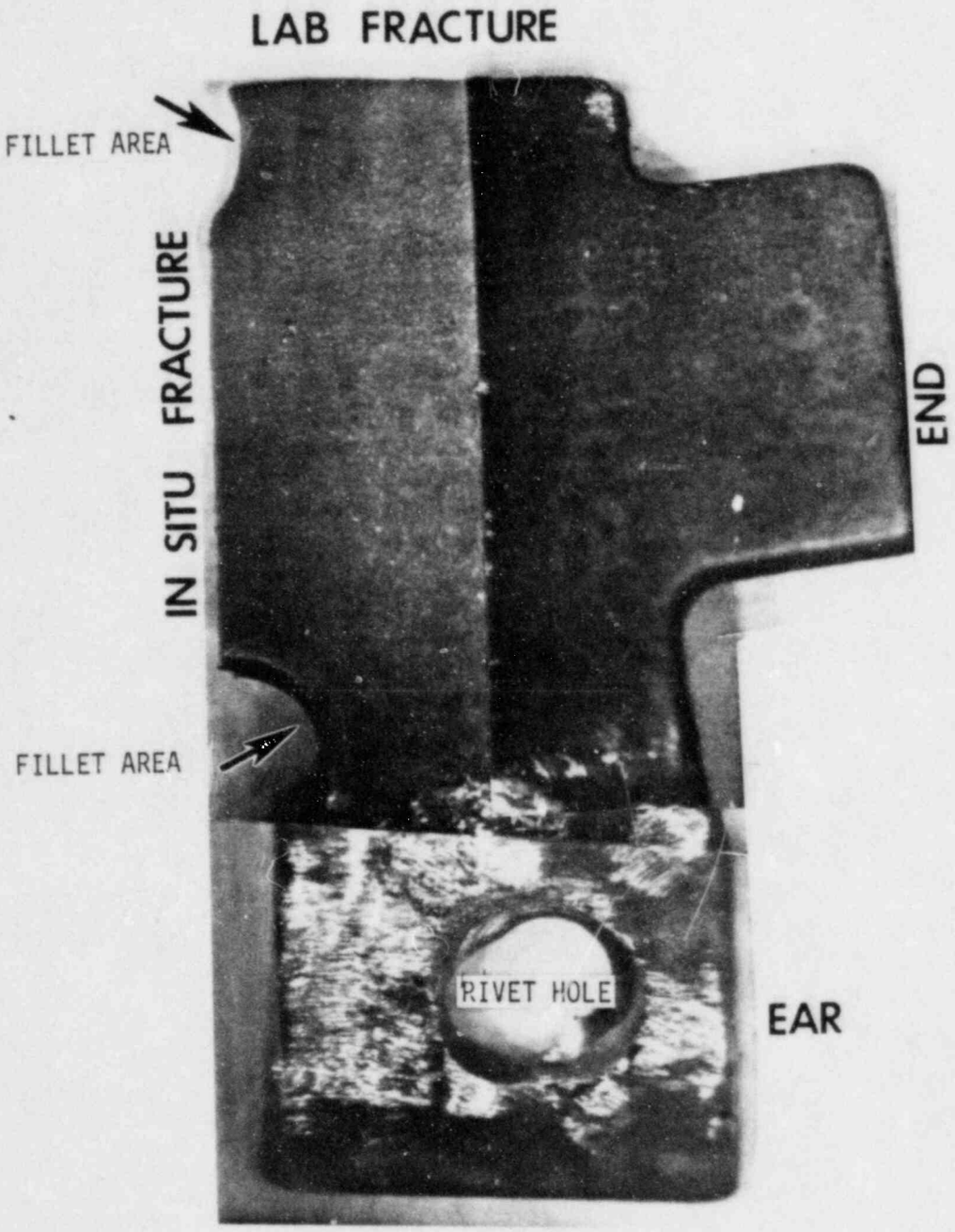

Figure 15 - Photomacrograph of the Top Side of the Large End of Spring DB-5 after Removal From the Nut. 1.75X

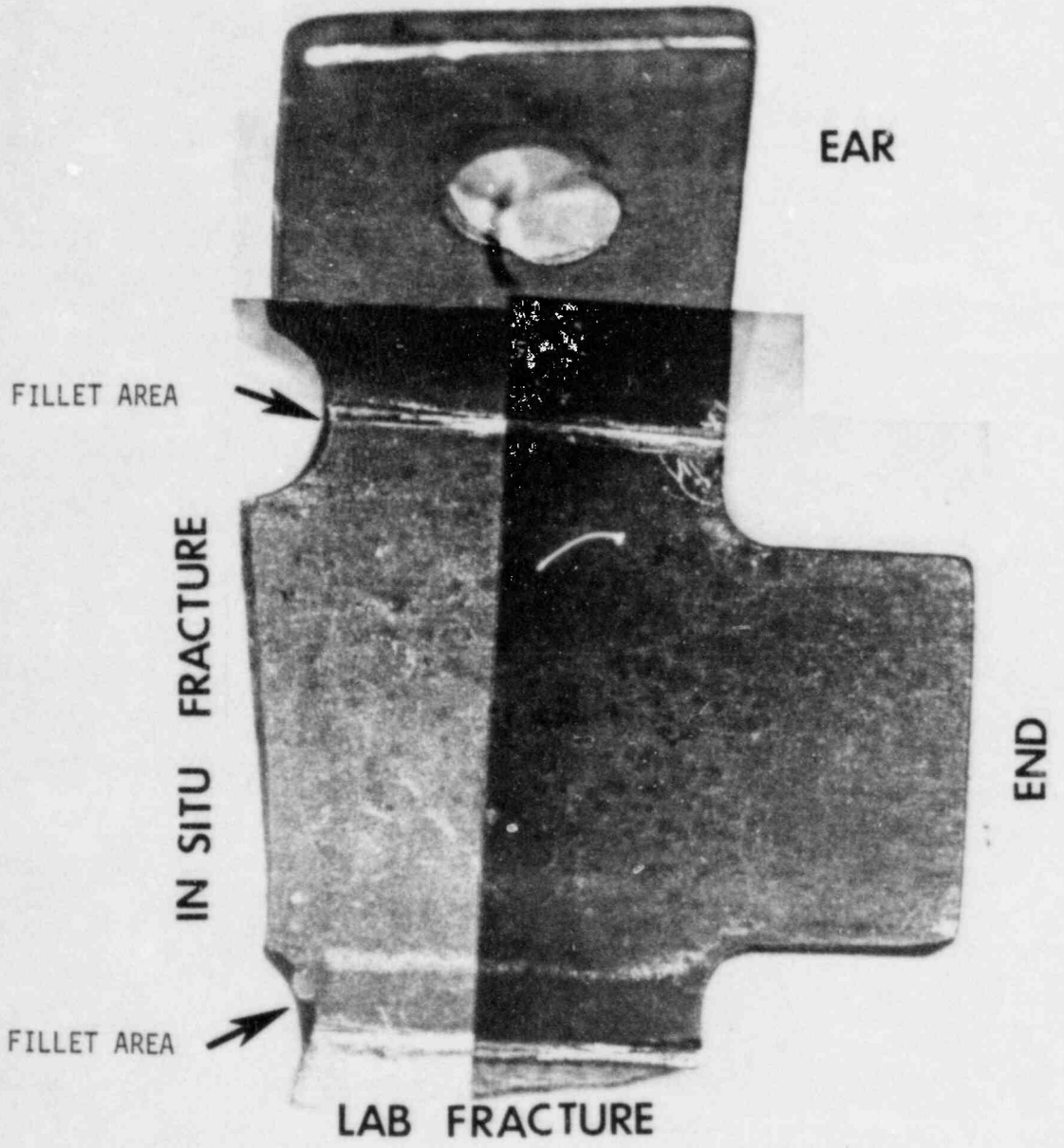

Figure 16 - Photomacrograph of the Bottom Side of the Large End of Spring DB-5 after Removal From the Nut. 1.75X

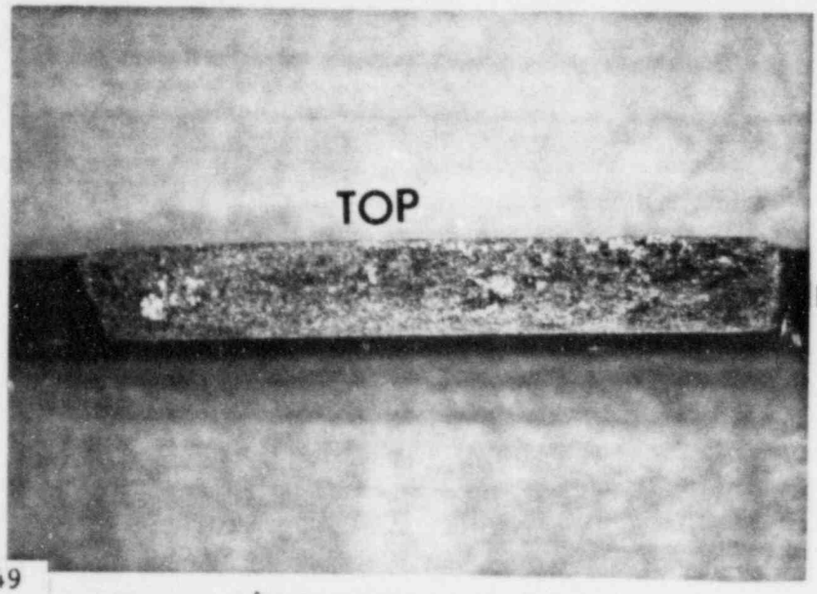

F85-49

Figure 17 - Fractograph of the Fracture from the Large End of DB-5. Mating Surface to Fracture "A" in Figure 12.

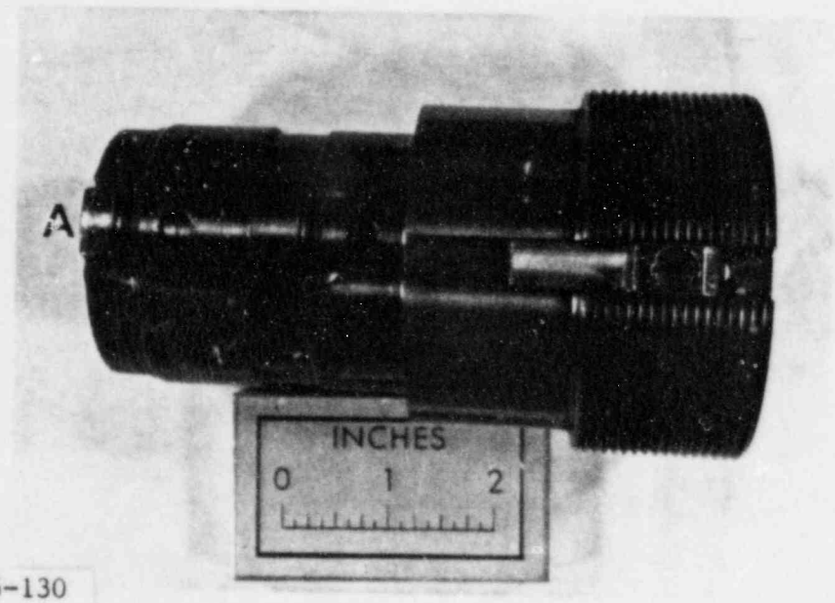

F85-130

Figure 18 - Photomacrograph of the Side View of CRDM Part # 706329-1145, Torque Tube Cap from Core Location E-3. 0.5X.

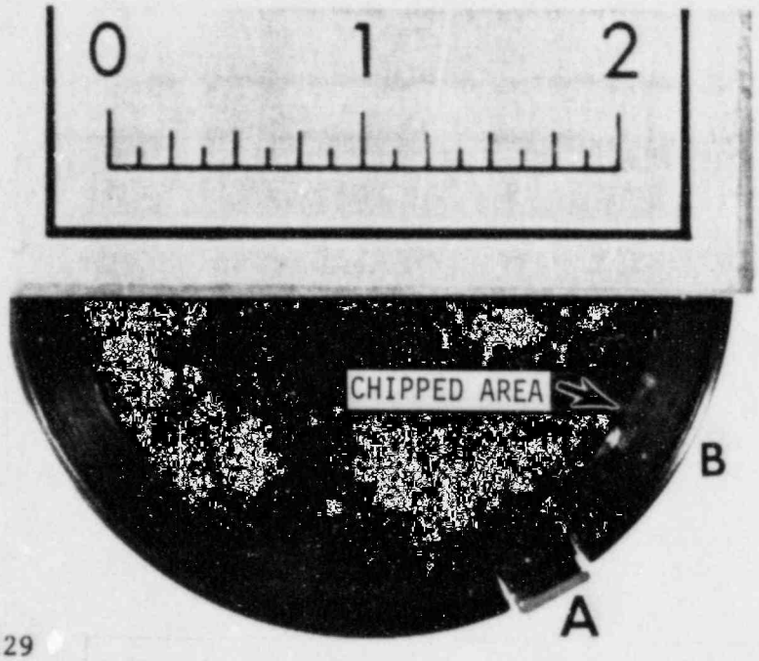

F85-129

Figure 19 - Photomacrograph Showing a Chipped Area on the Small End of the Torque Tube Cap in Figure 18. 1.3X.

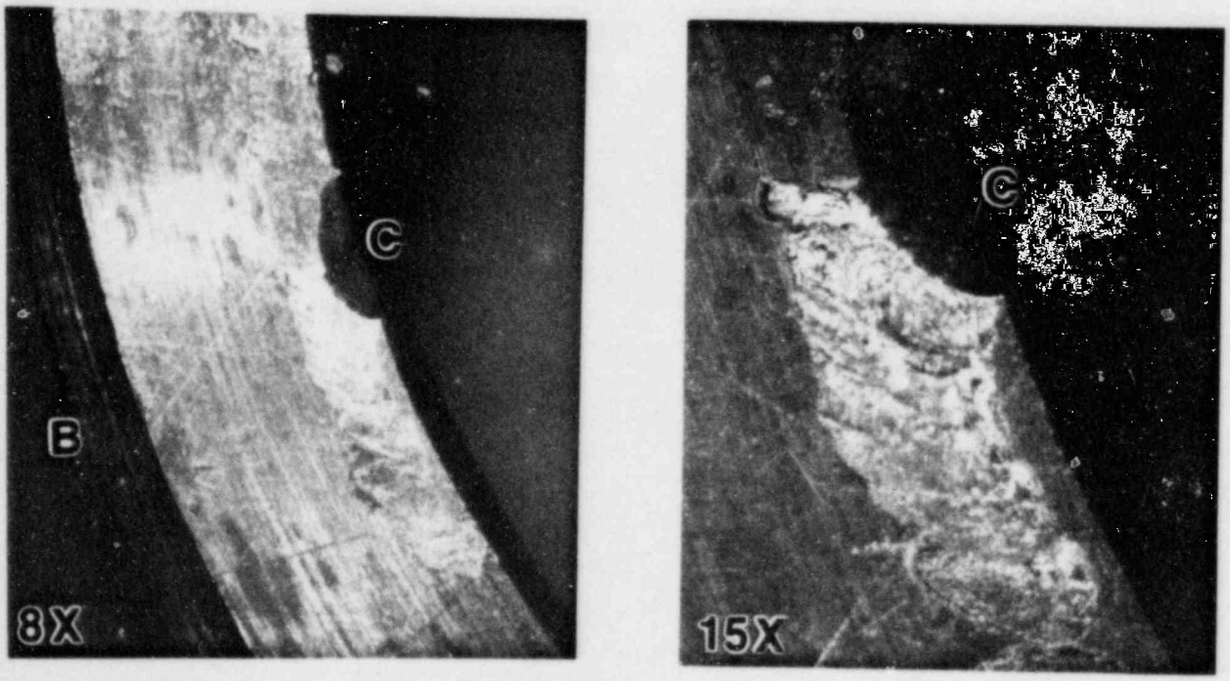

Figure 20 - Higher Magnification Views of the Chipped Area in Figure 19.

F85-132

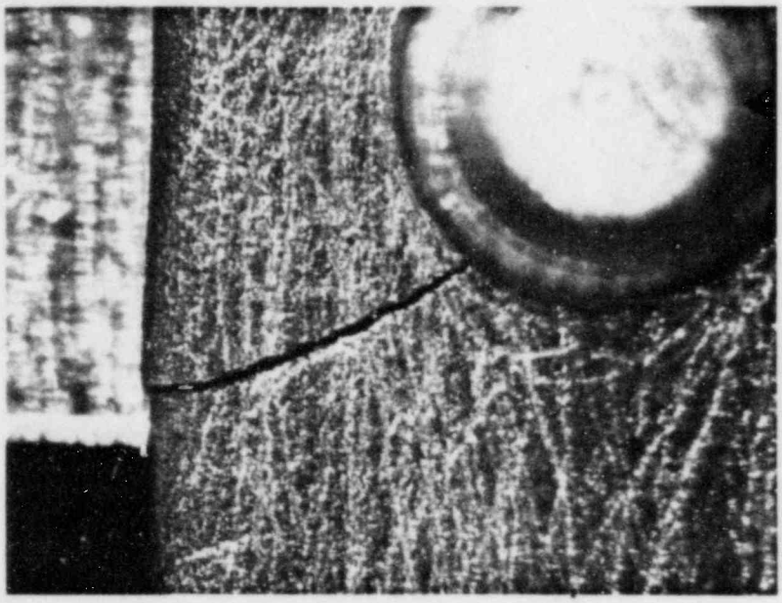

Figure 21 - Photomicrograph of the Crack at the Second Rivet Hole Viewed From the Top of DB-10. 16X.
F85-90

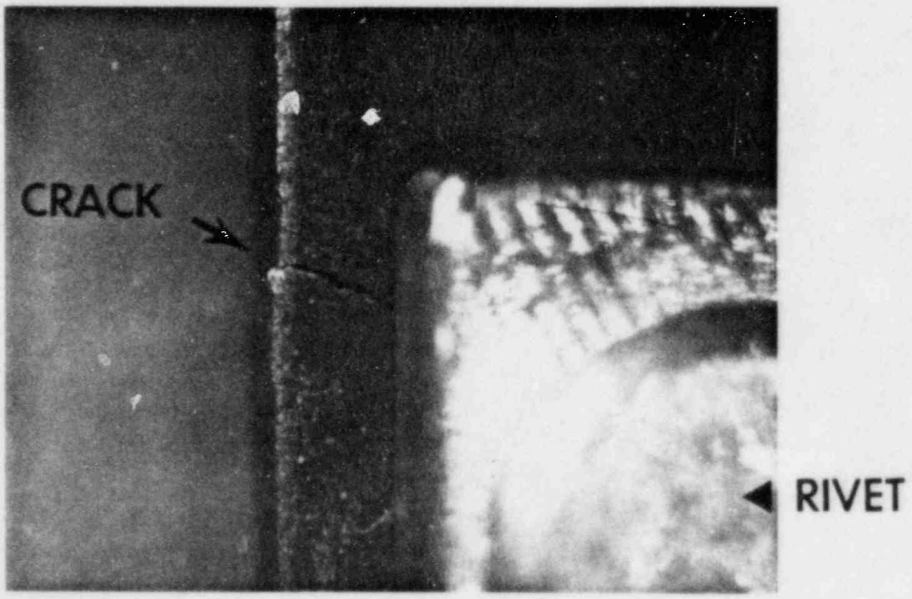

Figure 22 - Photomicrograph of the Bottom of Spring DB-10, Showing the Crack at the Second Rivet Hole. 14X.
F85-105

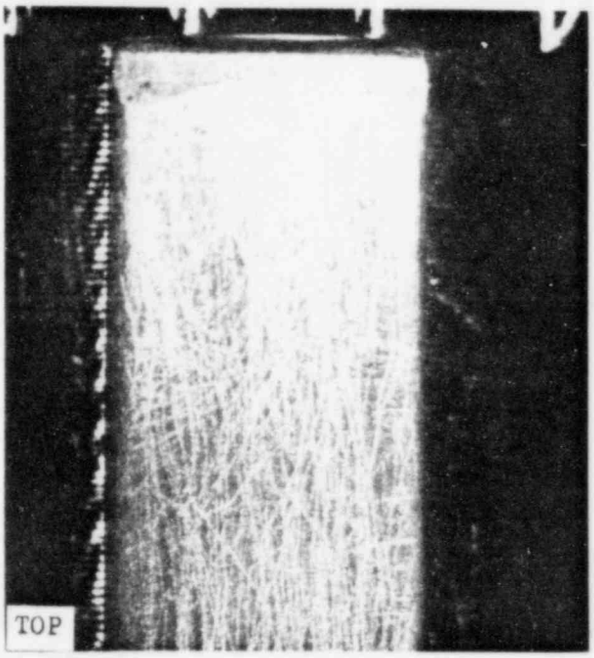

F85-81

F85-96

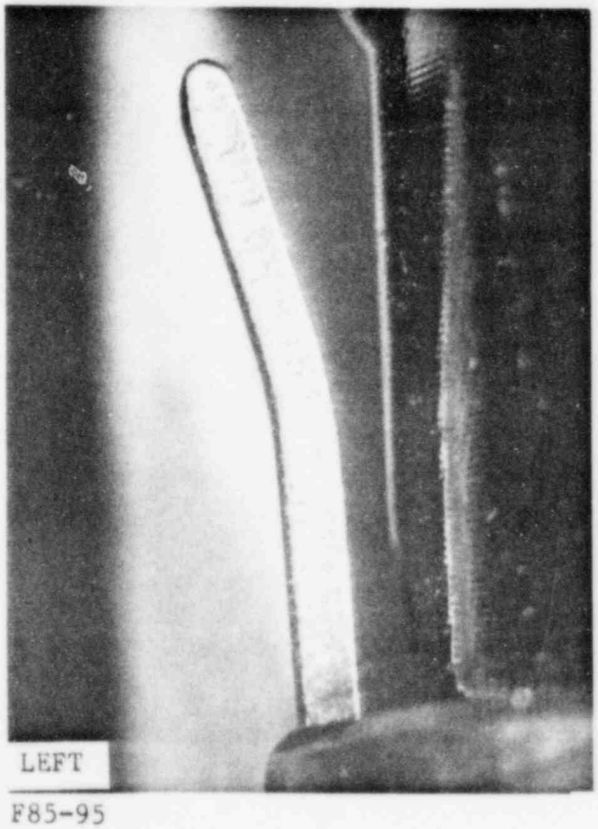

F85-95

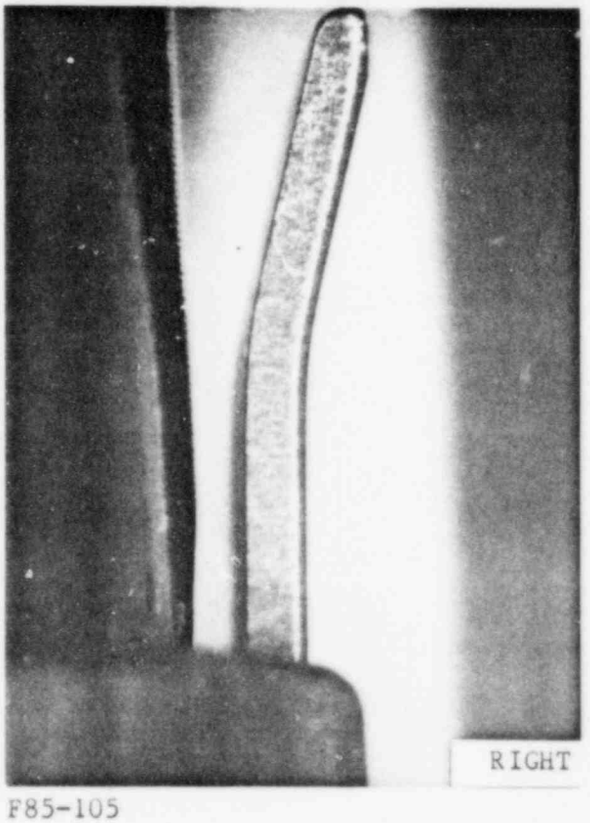

F85-105

Figure 23 - Photomacrographs Showing Four Orientations of the End of Spring Db-10. 6X.

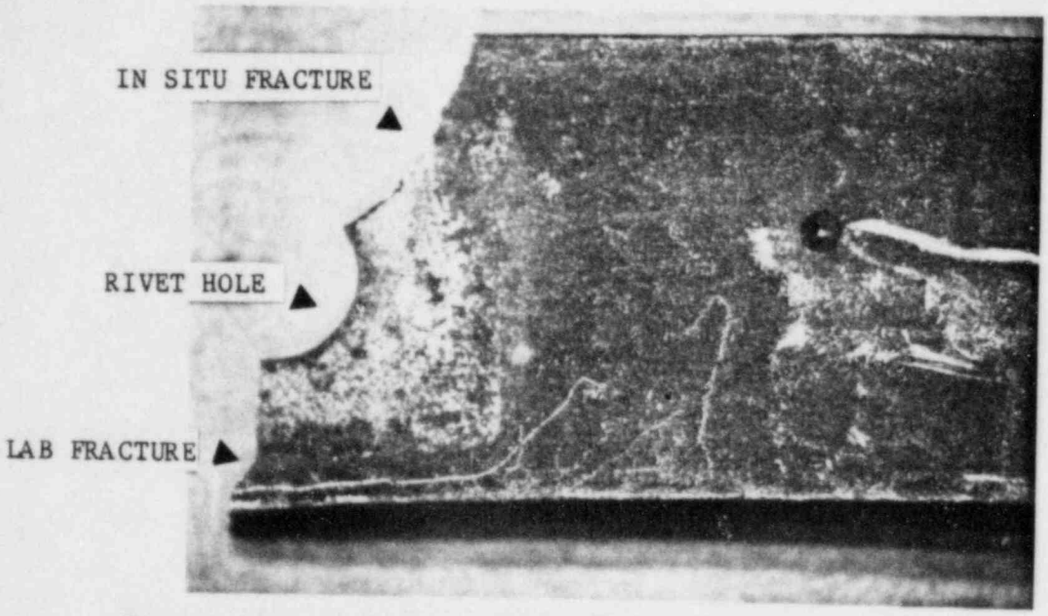

Figure 24 - Photomacrograph of the Bottom View of the Fracture in Spring DB-10 After Removal and Fracturing the Remaining Ligament. 8X.
F85-116

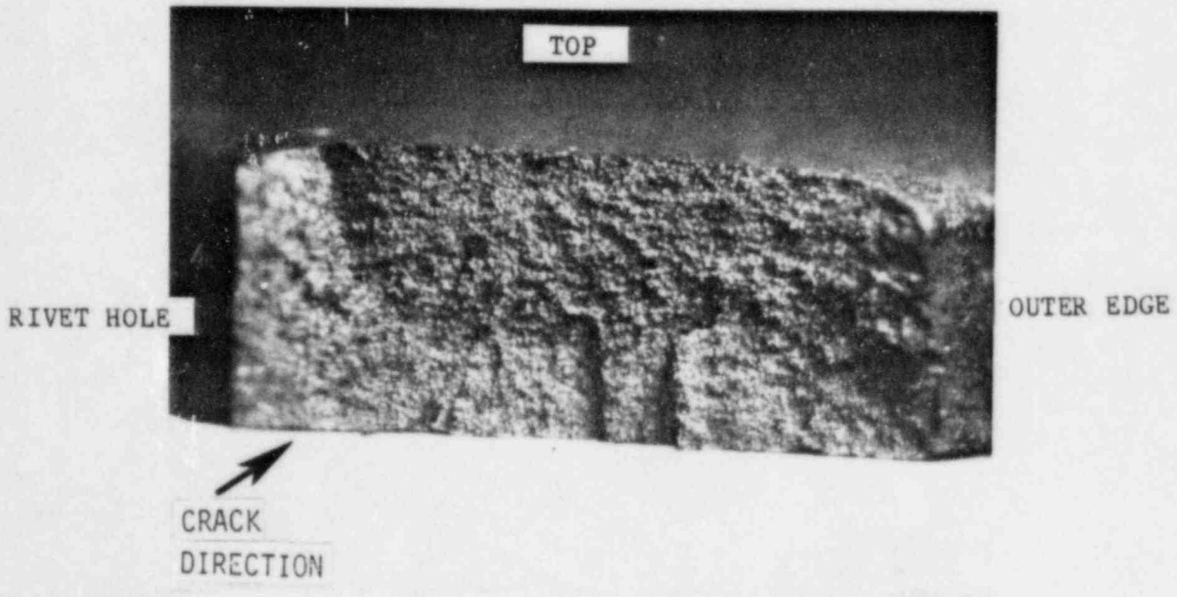

F85-112
Figure 25 - Fractograph of the In Situ Fracture in Spring DB-10. 24X.

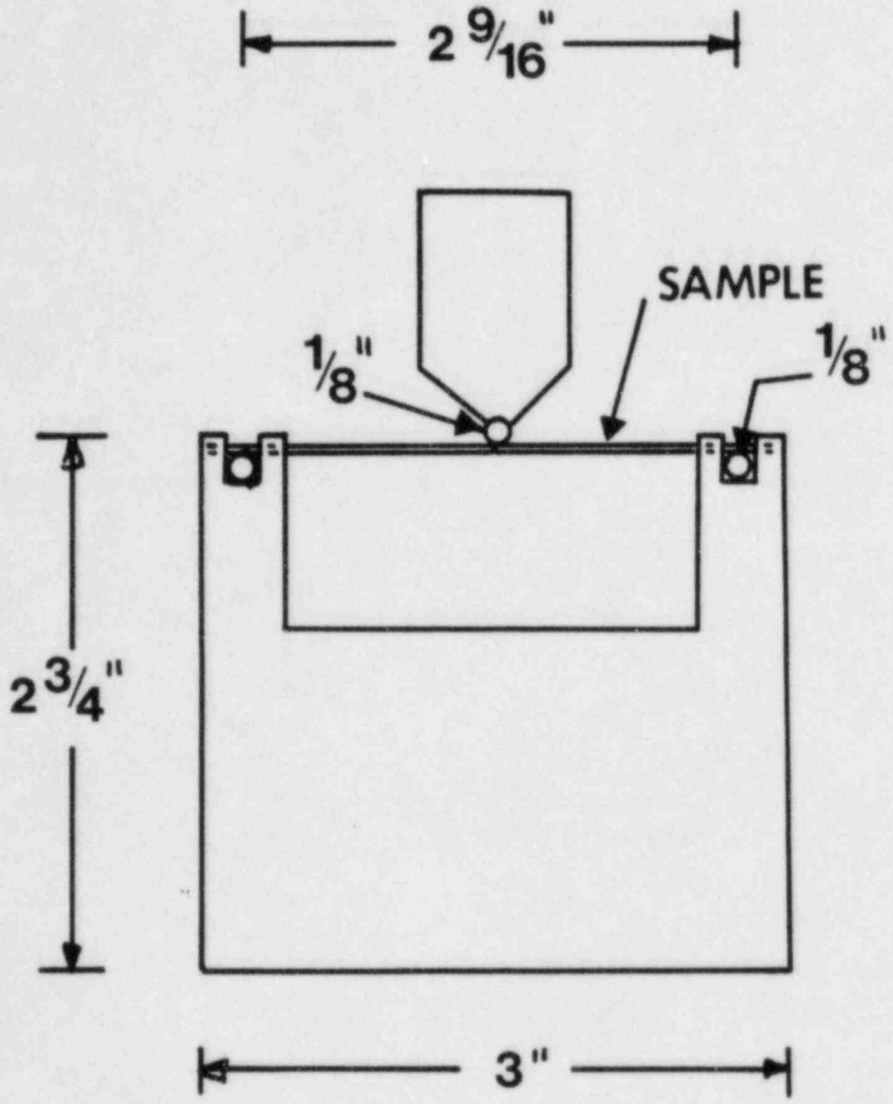

Figure 26 - Sketch Showing the Configuration of the Bend Test Fixture.

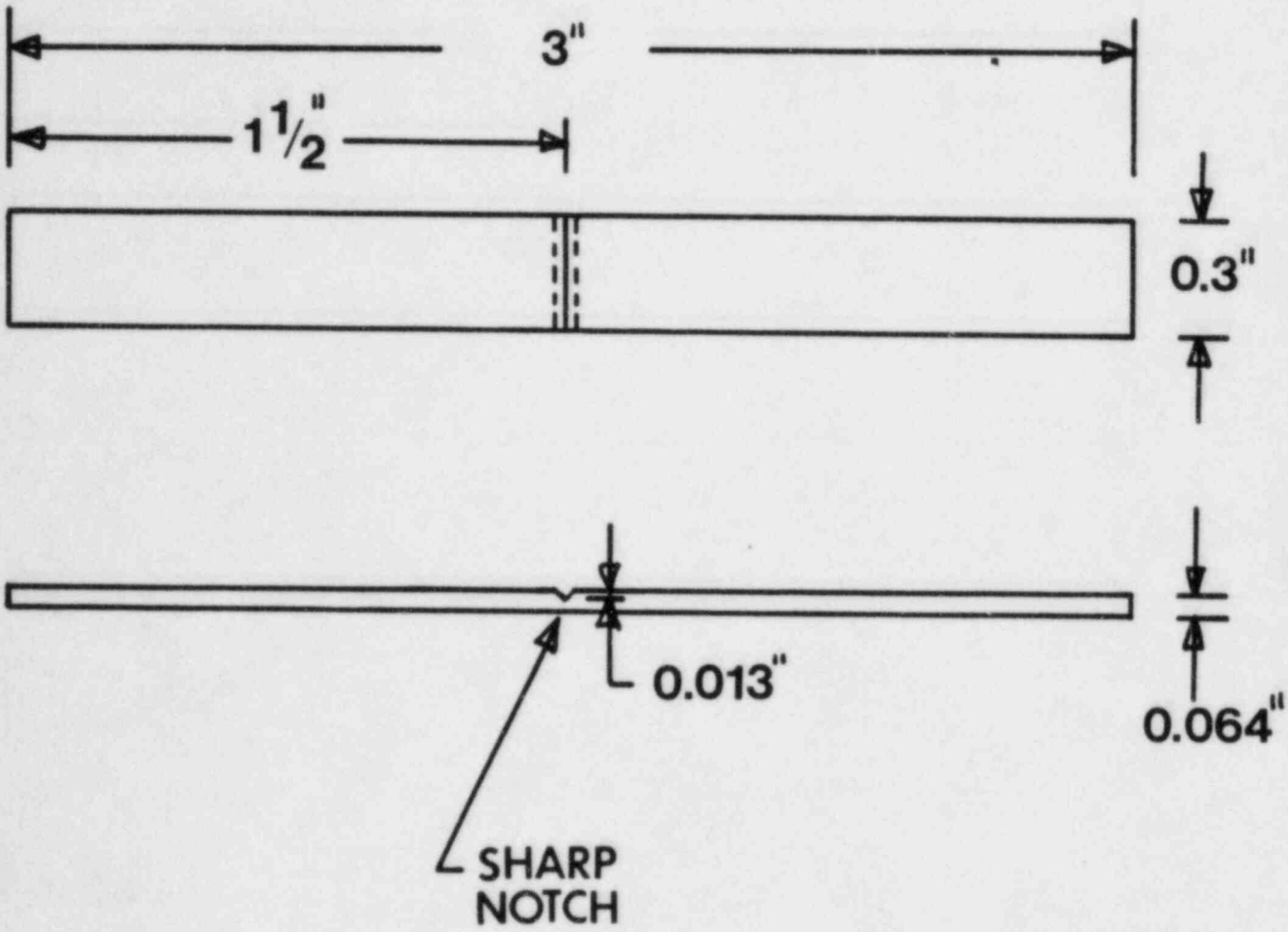

Figure 26 (cont.) - Sketch Showing the Configuration of the Bend Test Specimen. All Dimensions are Nominal. Actual Dimensions were Recorded. Not Drawn to Scale.

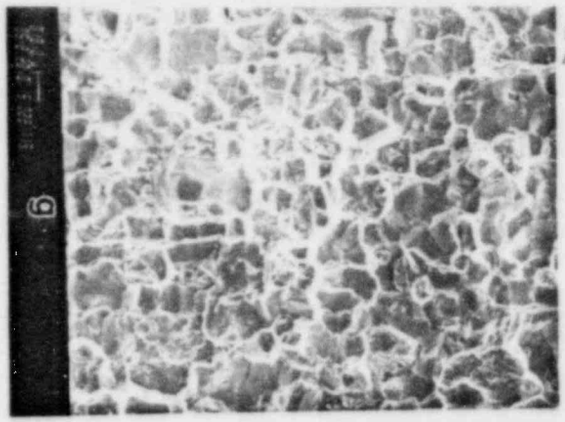

DB-5 LOCATION A
AFTER CLEANING

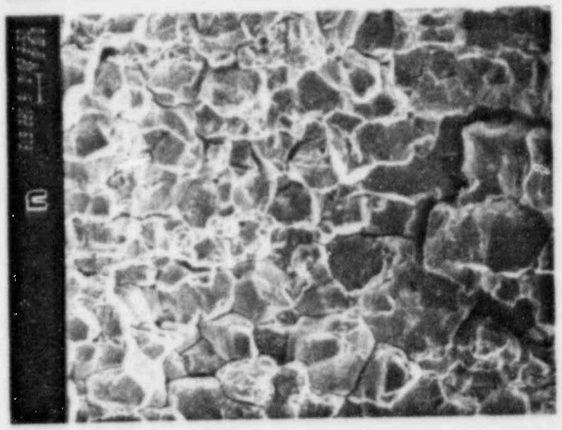

DB-5 LOCATION B
AFTER CLEANING

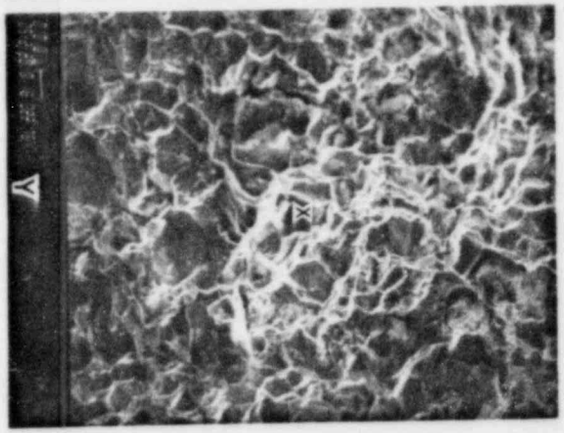

DB-10 BEFORE
CLEANING

Figure 27 - Comparison of Service and Laboratory Fracture Morphologies of Spring DB-5 and 10.

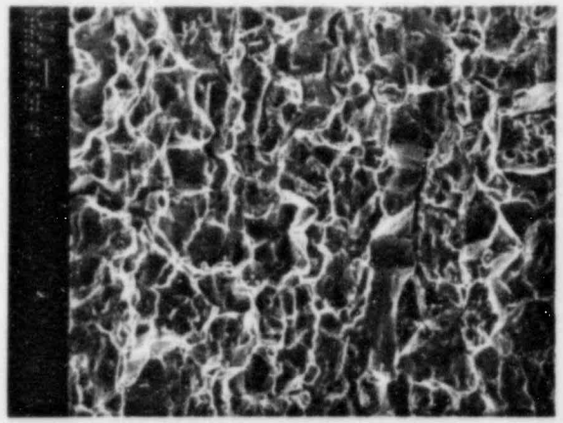

DB-5 NOTCHED LAB FRACTURE IN AIR

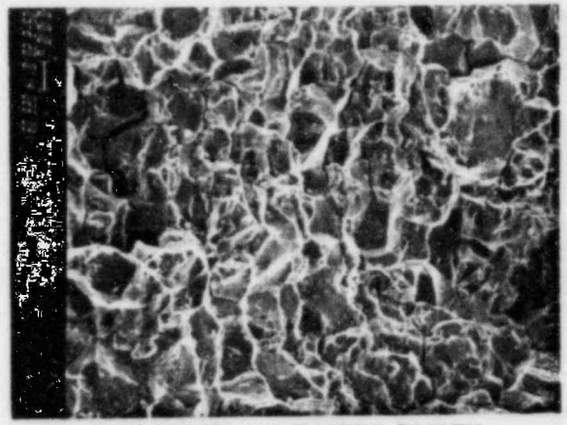

DB-13 NOTCHED LAB FRACTURE IN WATER
STRAIN RATE OF 3 INCHS/SECOND

DB-10 NOTCHED LAB FRACTURE IN AIR

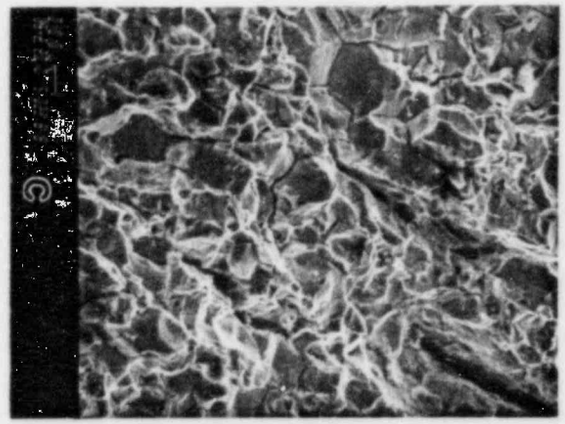

DB-10 NOTCHED LAB FRACTURE IN WATER
STRAIN RATE OF 0.5 INCHES/SECOND

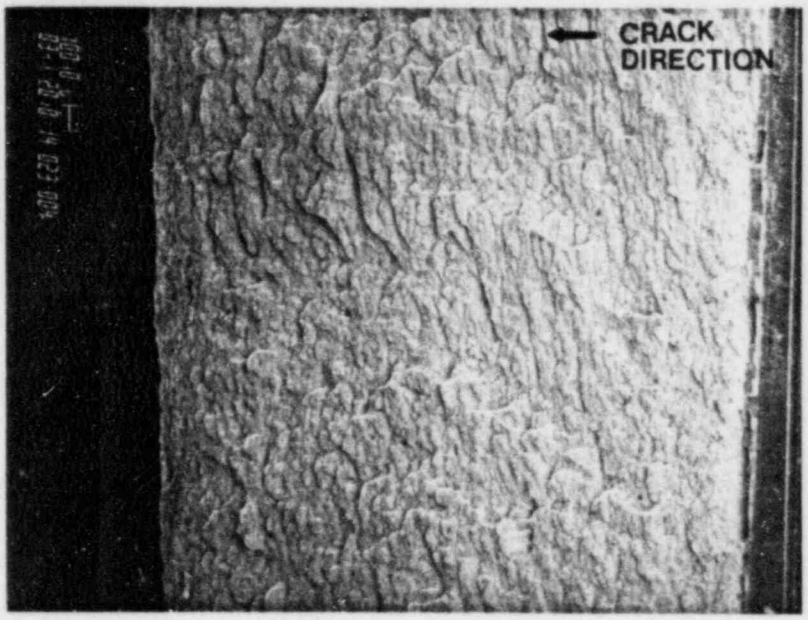

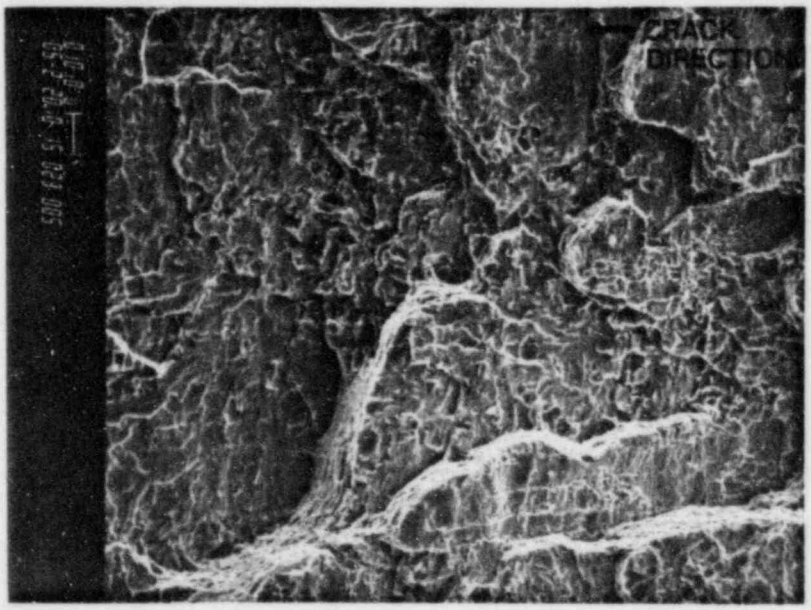

Figure 28 - SEM Fractograph of Three Point Bend Laboratory Fracture in Spring DB-11 from Heat 610073 Showing Quasi-Cleavage and Microvoid Coalescence.

NOTCH

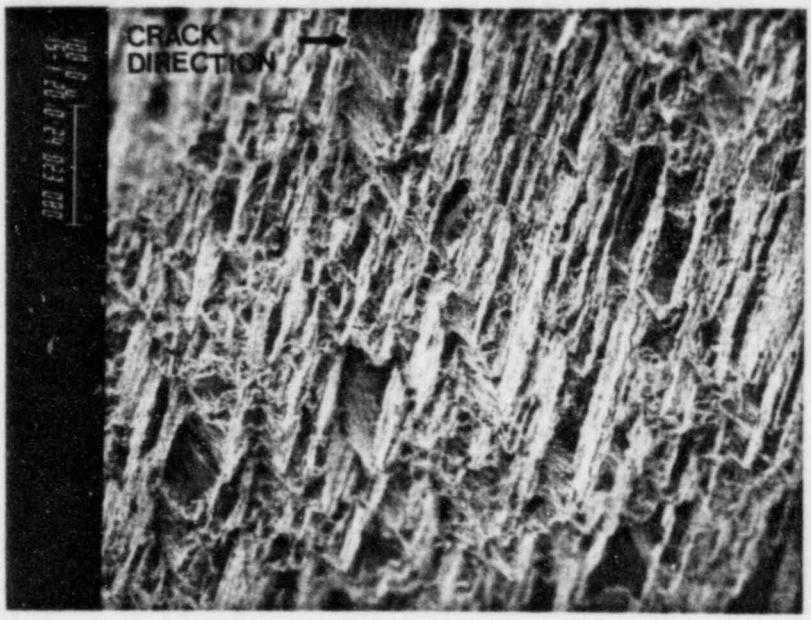

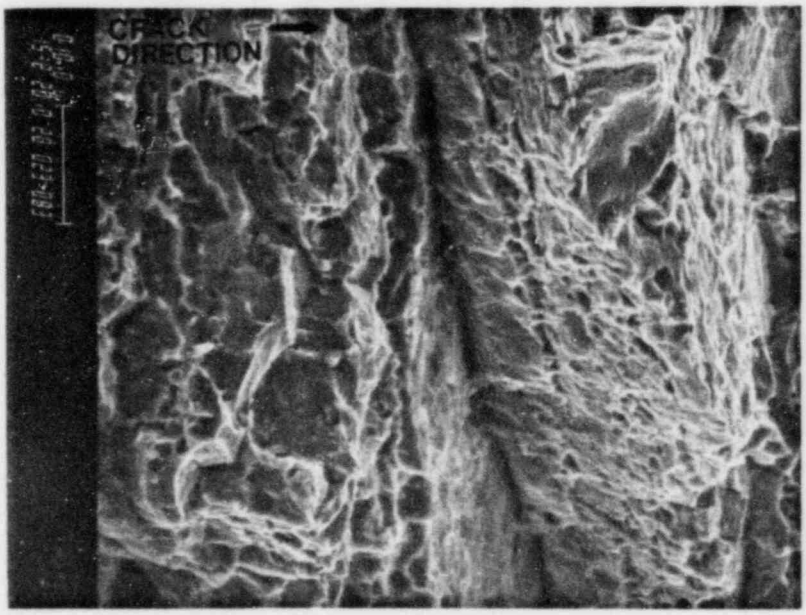

Figure 29 - SEM Fractograph of Three Point Bend Laboratory Fracture in Spring DB-12 from Heat 610073 Showing Quasi-Cleavage and Microvoid Coalescence.

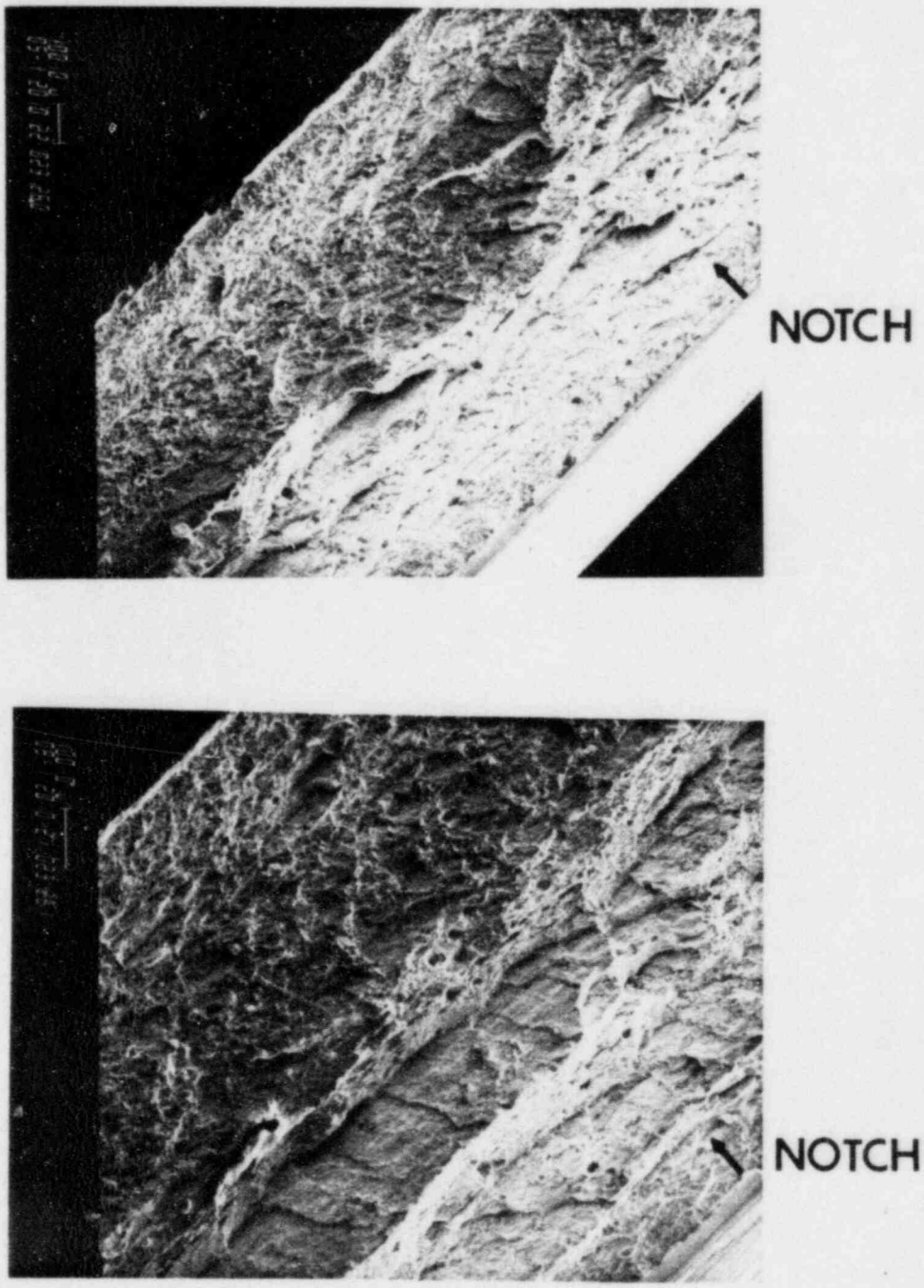

Figure 30 - SEM Fractographs of Three Point Bend Laboratory Fracture in Spring DB-14 from Heat 230232 Showing Ductile Rupture - Microvoid Coalescence

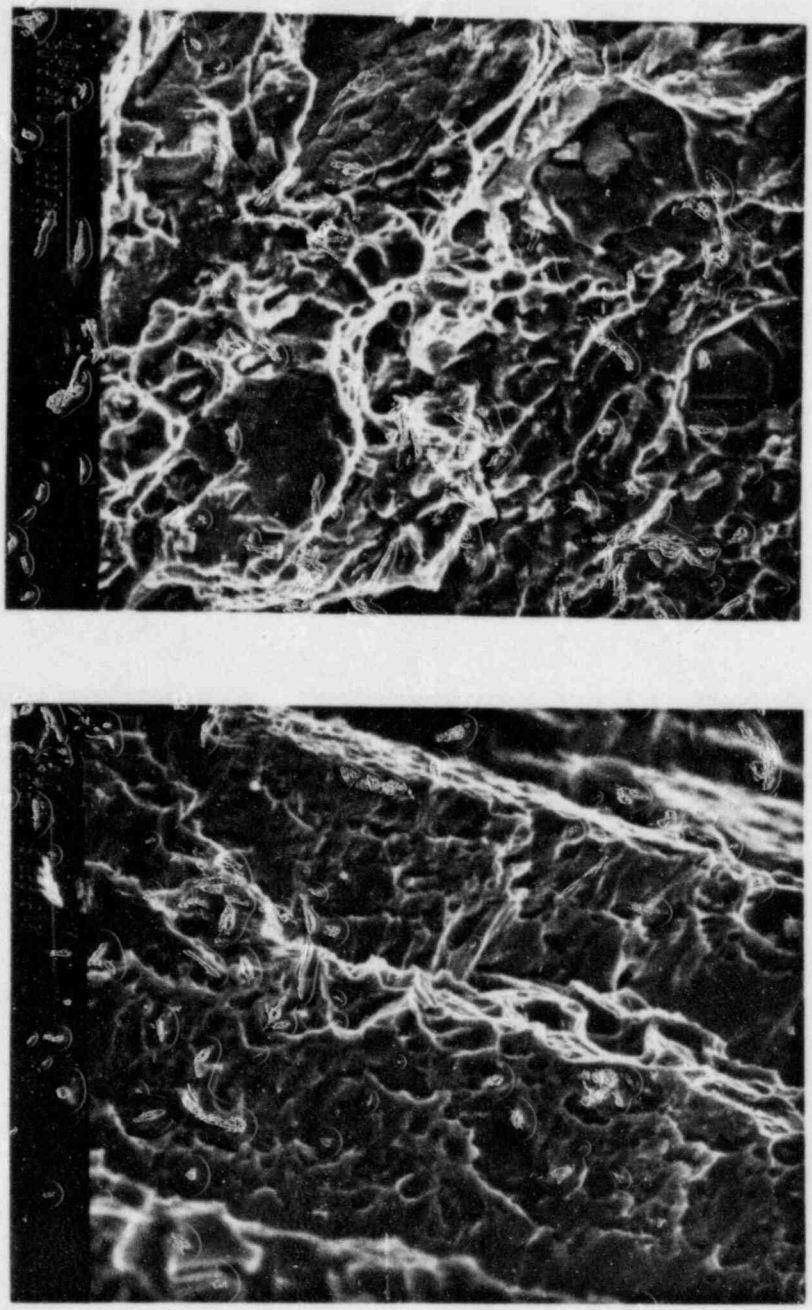

Figure 31 - Higher Magnification Views of Ductile Rupture in Figure 30.

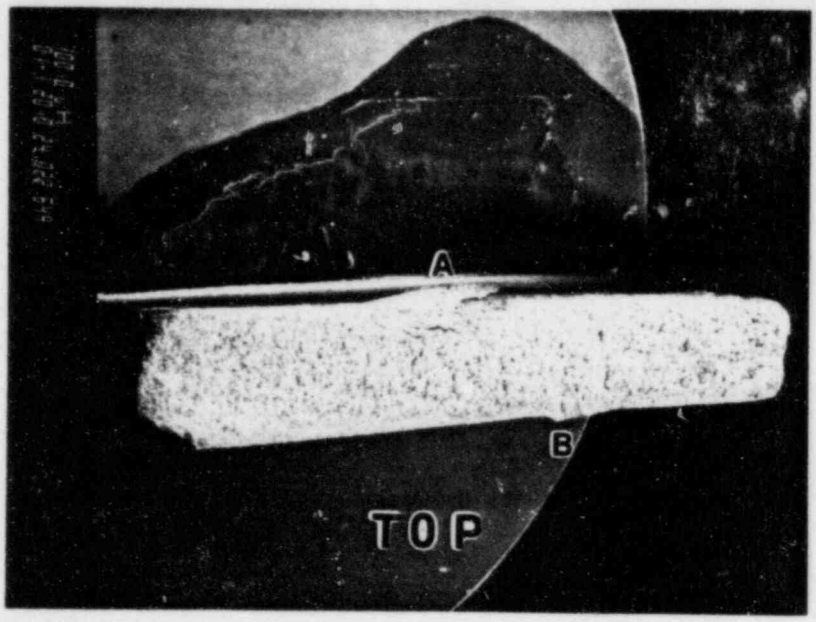

Figure 32 - SEM Fractograph of In Situ Fracture "A" in Spring DB-5.

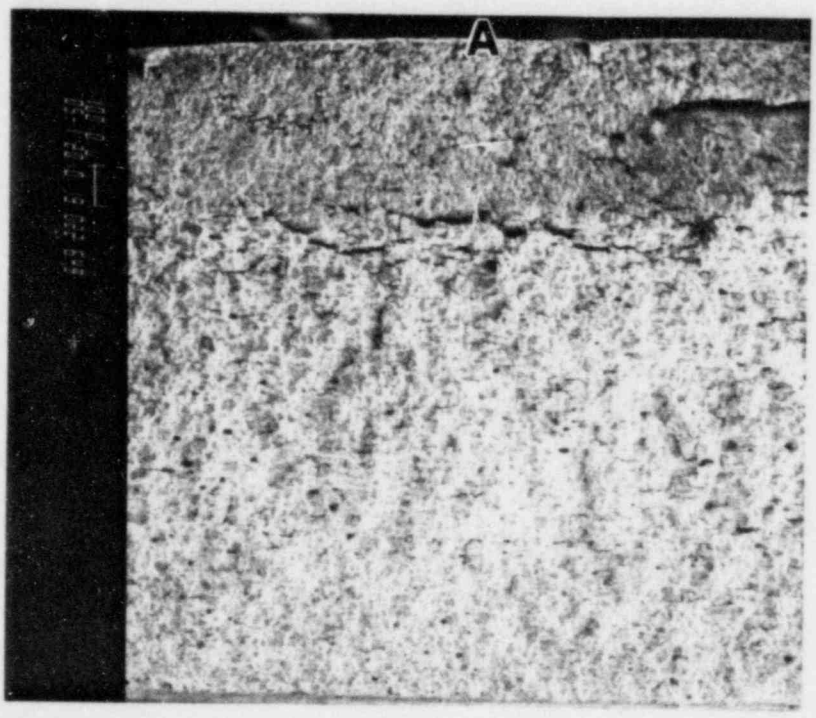

Figure 33 - SEM Fractograph of Impact Area "A" in Figure 32.

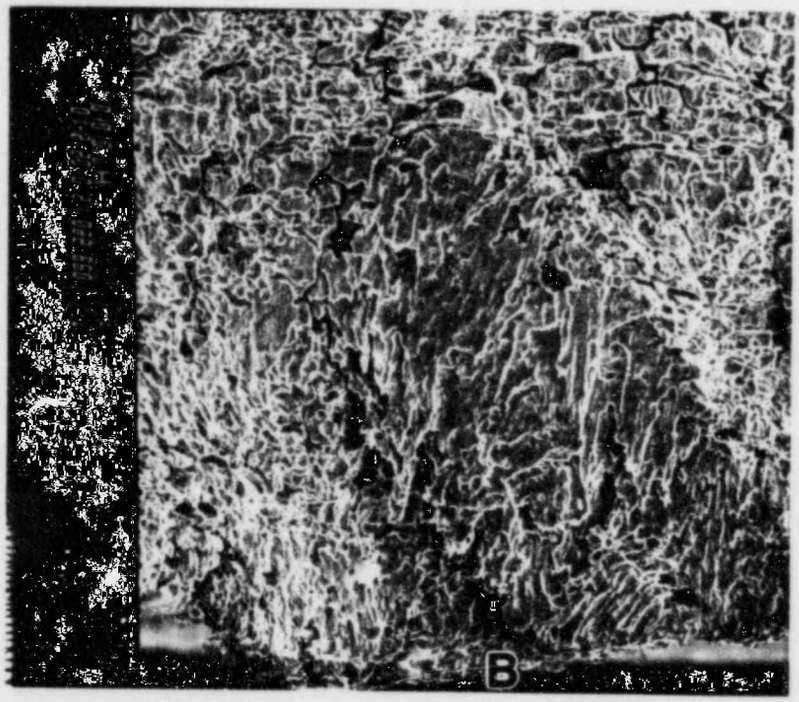

Figure 34 - SEM Fractograph of Area "B" in Figure 32 Showing Localized Deformation.

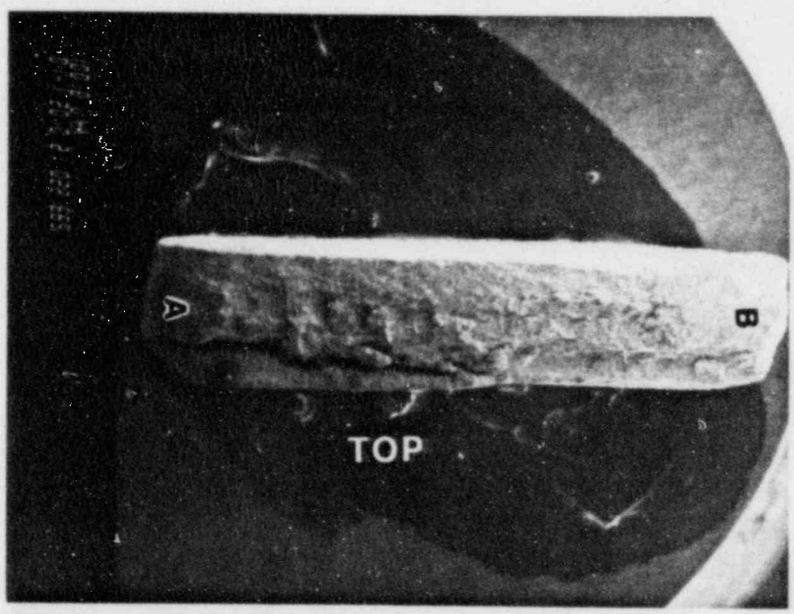

Figure 35 - SEM Fractograph of the Small End In Situ Fracture (B) on Spring Sample DB-5 Large cracks and Two Impact Areas, "A" & "L", are Shown.

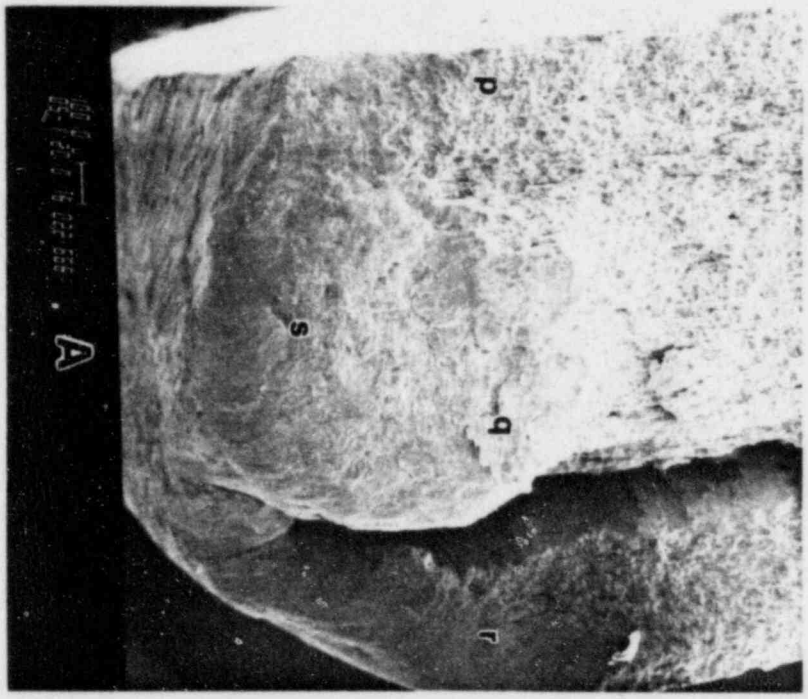

Figure 36 - SEM Fractograph of the Largest Impact Area, Area "A" and Secondary Cracking shown in Figure 35.

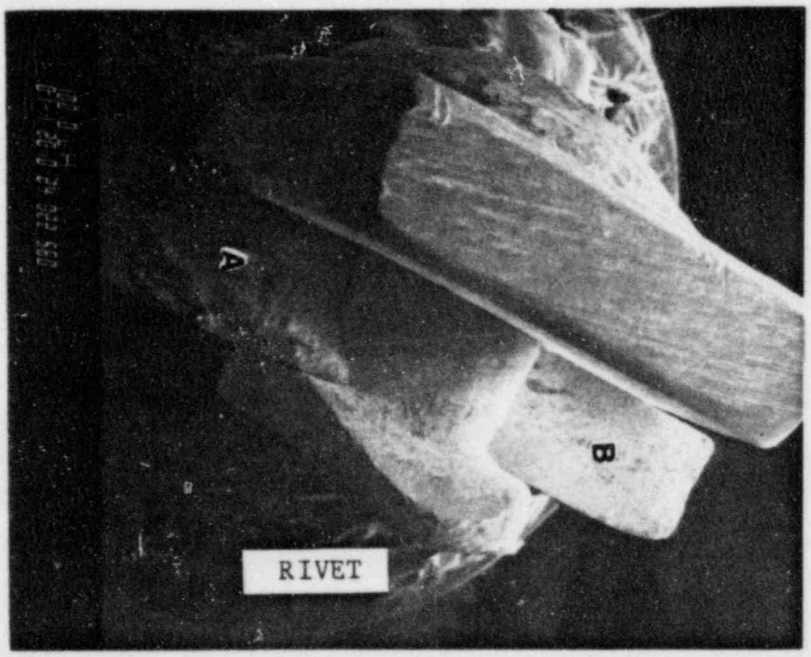

PIN ASSEMBLY

Figure 37 - SEM Fractograph of the In Situ Fractures in Spring Sample DB-6 Showing Rivet, Pin Assembly, and Fracture Surface

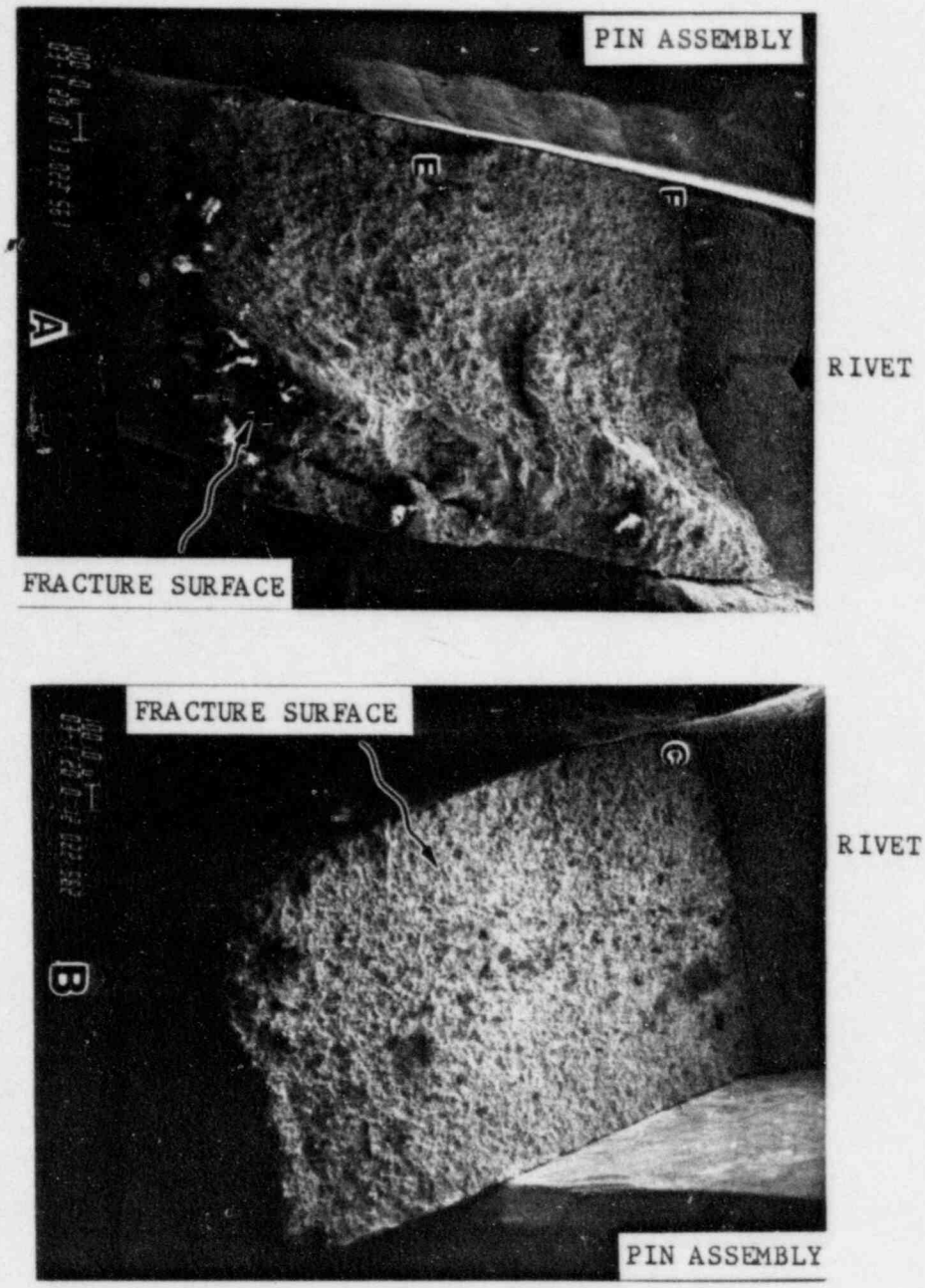

Figure 38 - Higher Magnification Views of In Situ Fractures in Figure 37

Figure 39 - SEM Fractograph of the Fracture Surface on Spring DB-10 showing the Rivet Hole and Lab and In Situ Fractures.

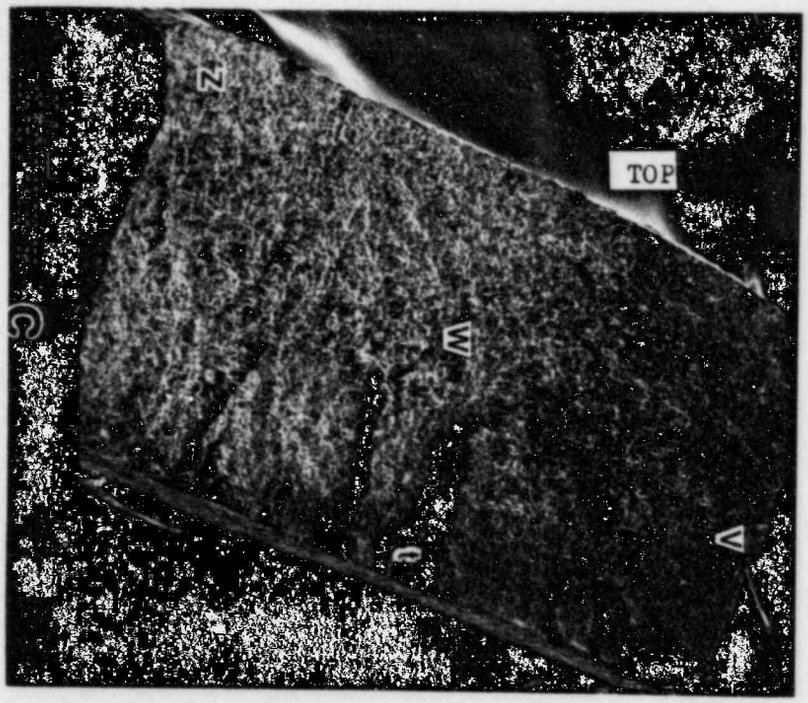

Figure 40 - SEM Fractograph of the IN Situ Fracture in Spring DB-10, Area "C" as Shown in Figure 39.

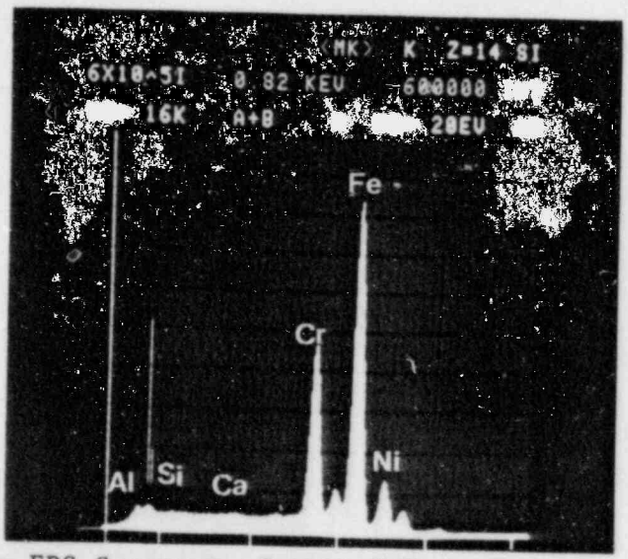

Figure 41 - EDS Spectrum of AREA "W" in Figure 40 Showing the Presence of AL, Si, Possible Ca, Cr, Fe, and Ni.

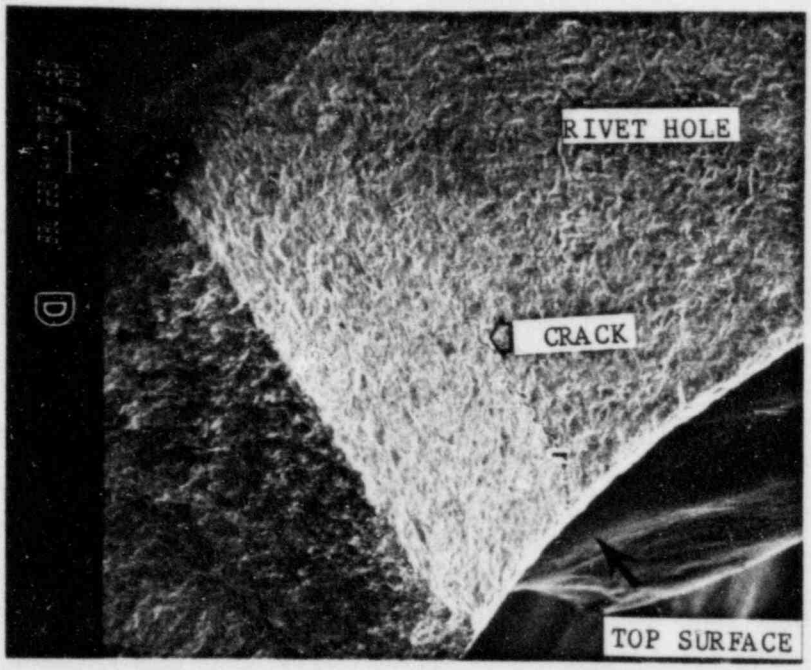

Figure 42 - SEM Fractograph of Area "D" in Figure 39 Showing a Crack in the Rivet Hole Area.

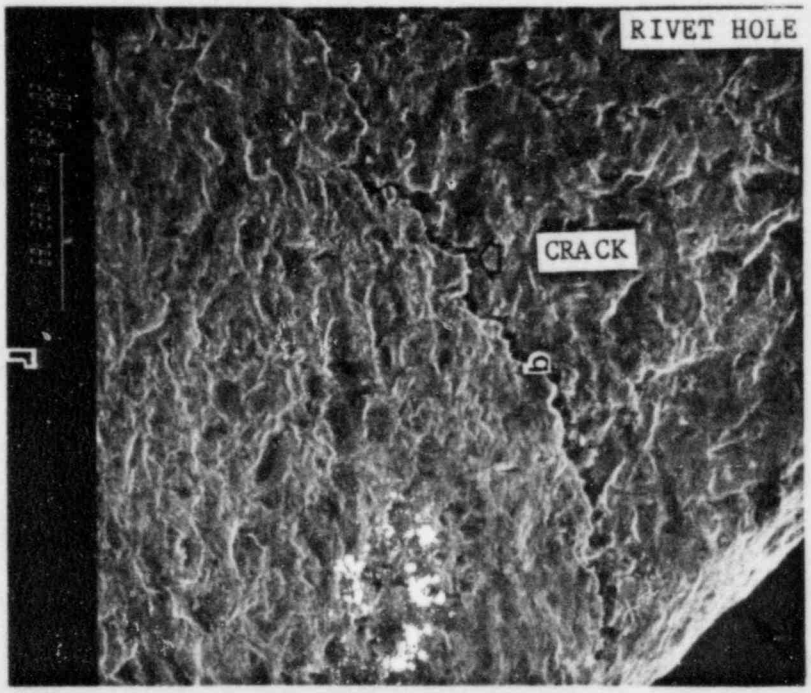

Figure 43 - SEM Fractograph of Area "r" in Figure 42.

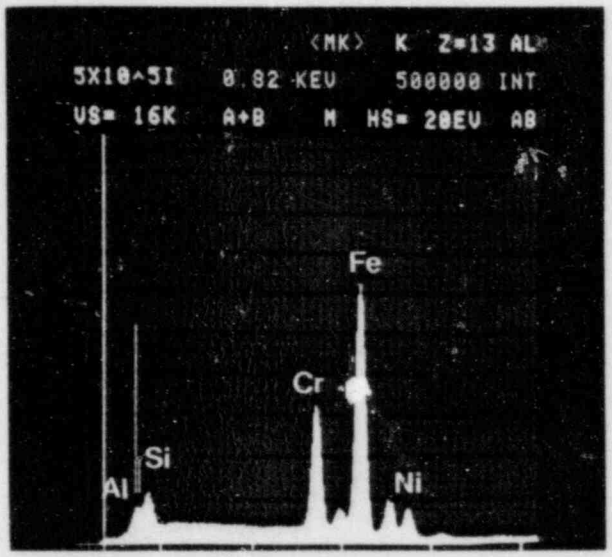

Figure 44 - EDS Spectrum of AREA "q" in Figure 43 Showing the Presence of AL, Si, Cr, Fe, and Ni.

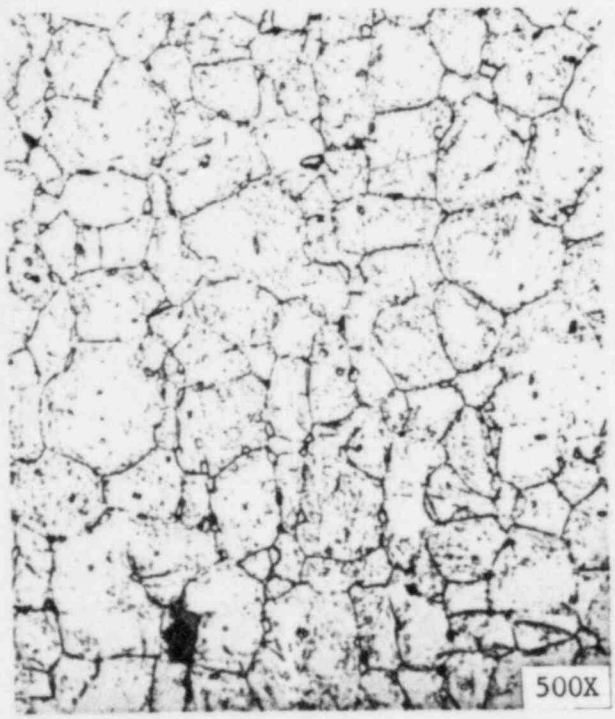

OPTICAL M85-165

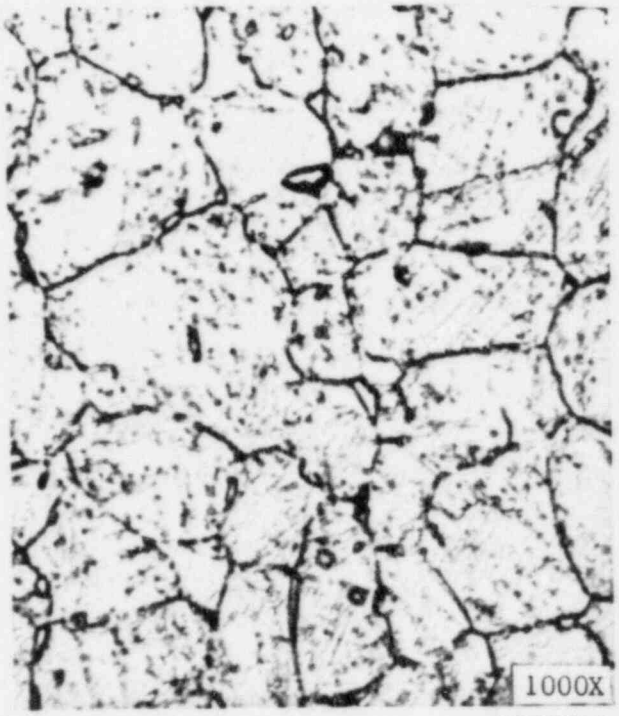

M85-166 OPTICAL

SECONDARY ELECTRON SEM IMAGE

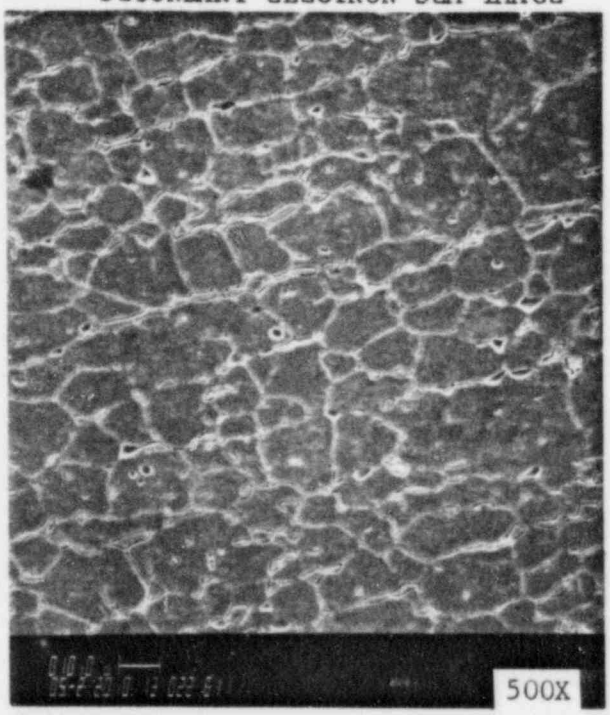

SECONDARY ELECTRON SEM IMAGE

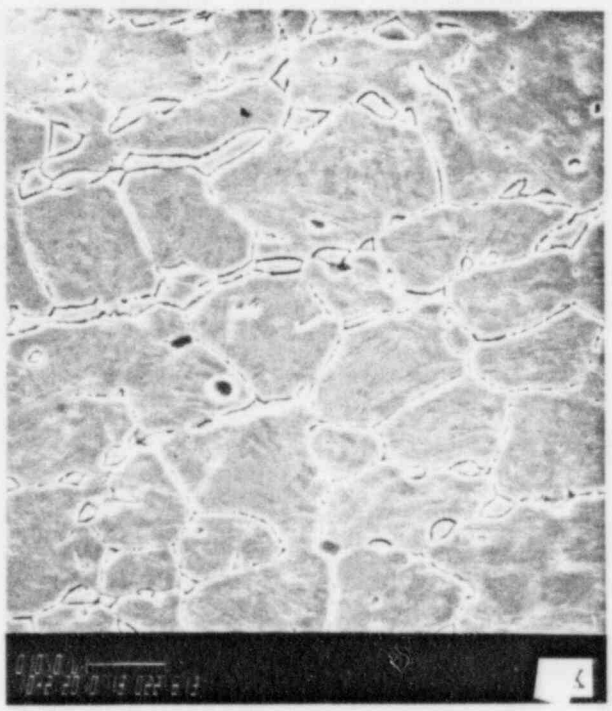

Figure 45 - Optical (Upper Row) and SEM (Lower Row) Photomicrographs of Spring DB-5 (Heat 300130) Showing Stringers and Globules of Ferrite and Carbide Networks in a Martensite Matrix. Electrolytic 10% Ammonium Persulfate Etch.

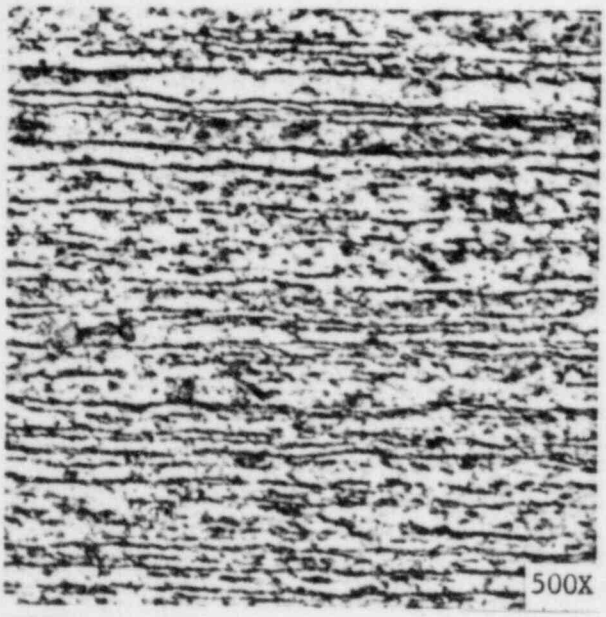

OPTICAL M85-191

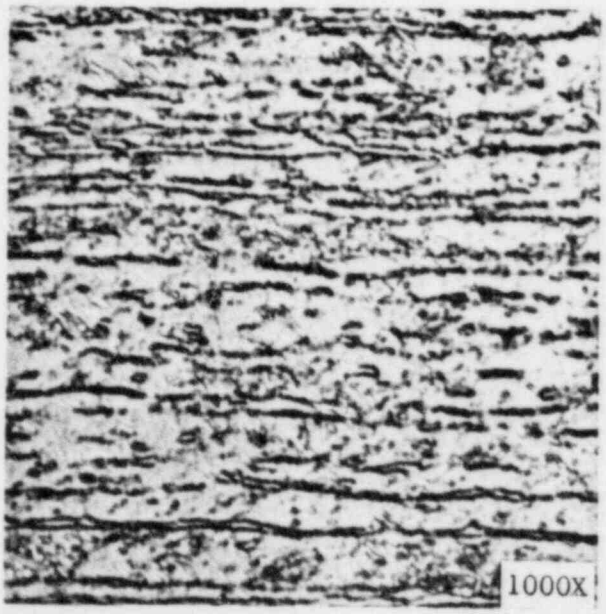

OPTICAL M85-192

SECONDARY ELECTRON SEM IMAGE

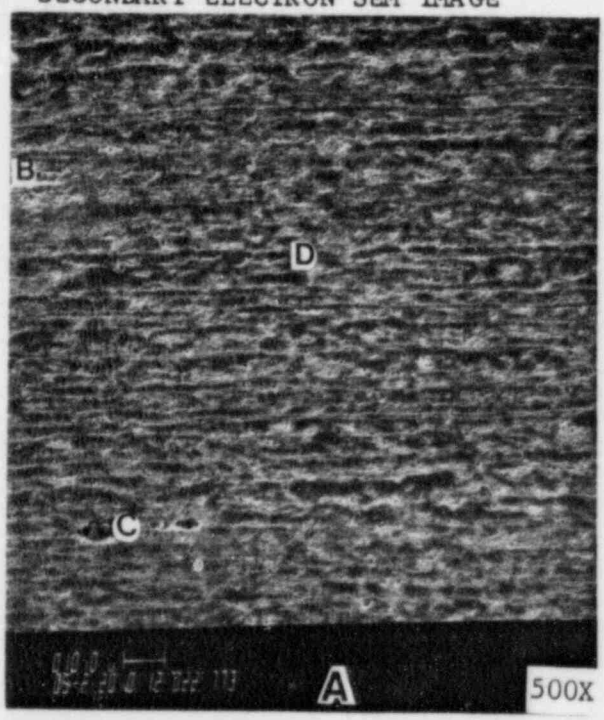

SECONDARY ELECTRON SEM IMAGE

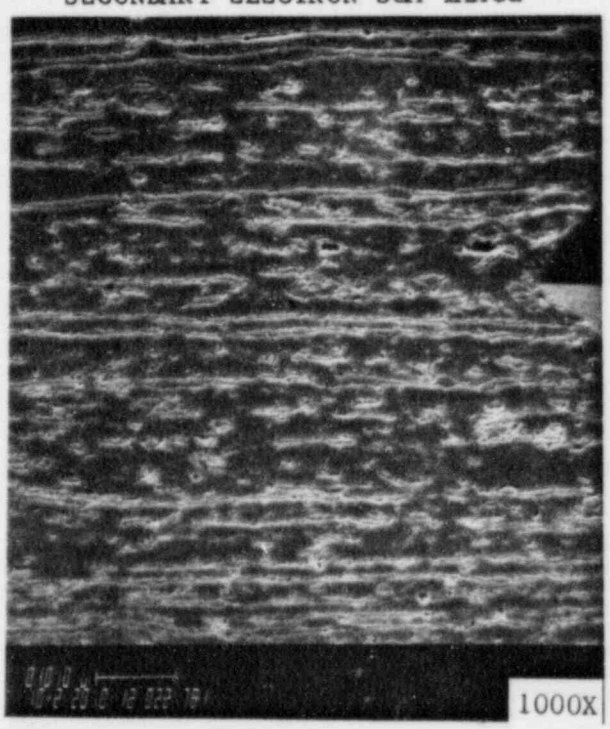

Figure 46 - Optical (Upper Row) and SEM (Lower Row) Photomicrographs of Spring DB-9 (Heat 610073) Showing Distorted Structure With Stringers and Globules of Ferrite and Carbide Networks in a Martensite Matrix. Electrolytic 10% Ammonium Persulfate Etch.

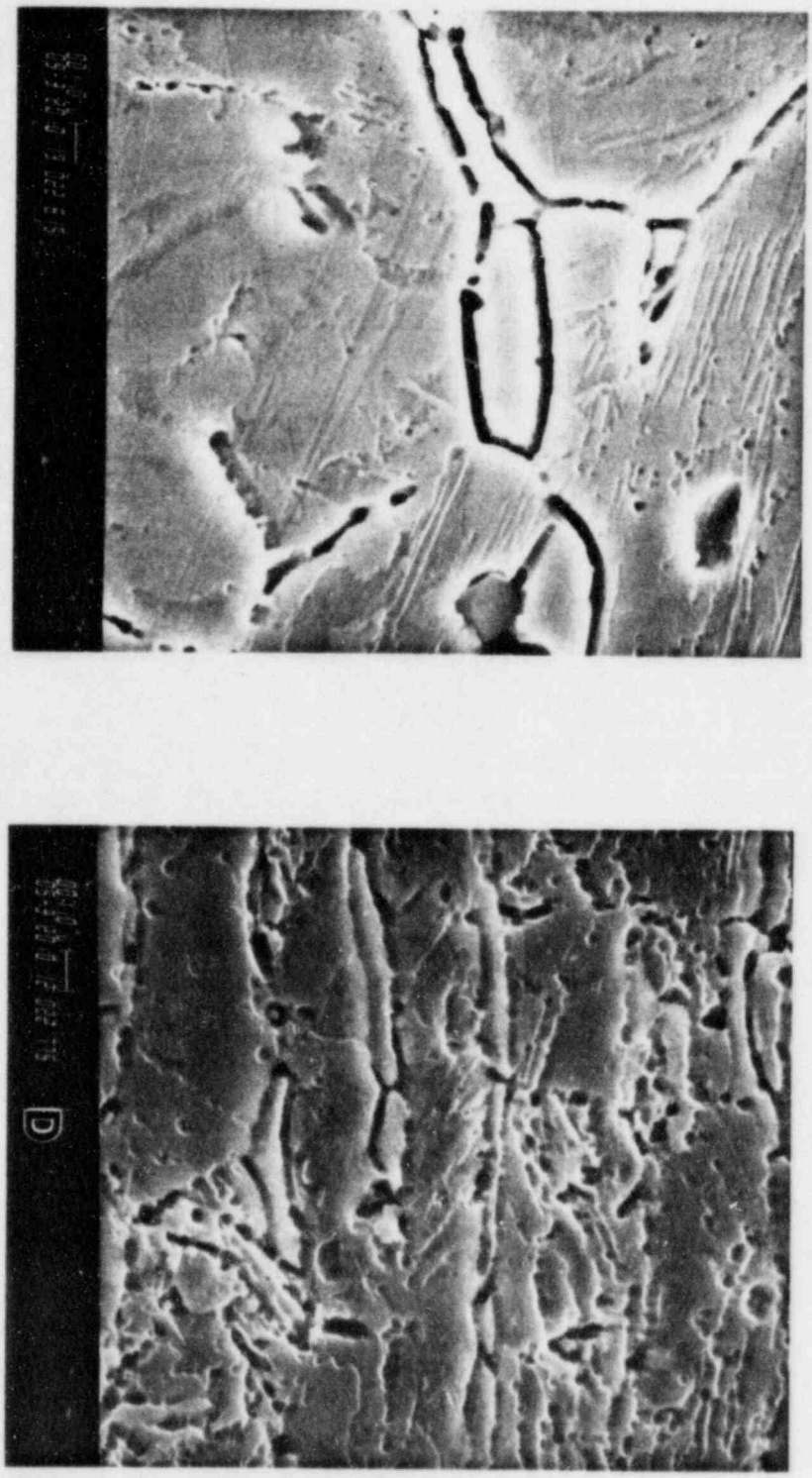

Figure 47 - Comparison SEM Photomicrographs From Heats 300130 and 610073 Showing the Difference in Carbide Distribution.

SPRING DB-10 HEAT 300130

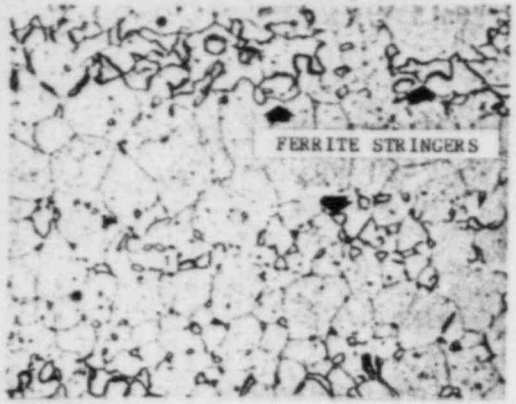

M85-262

SPRING DB-9 HEAT 610073

M85-303

TOP VIEW 500X
SPRING AXIS

M85-301

EDGE VIEW 500X
SPRING AXIS

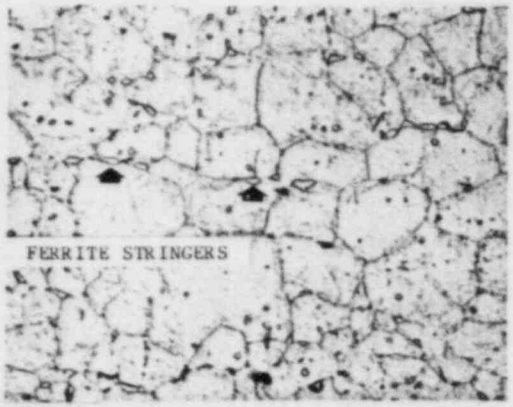

M85-261

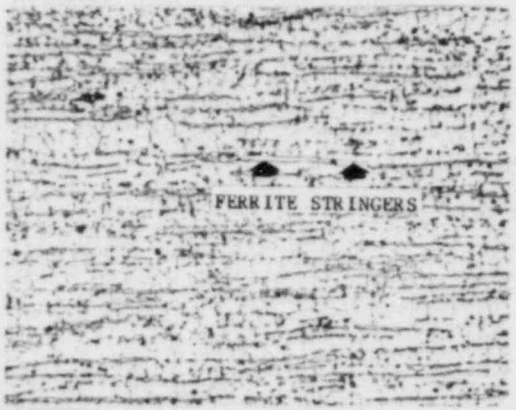

M85-299

END VIEW 500X
SPRING AXIS INTO PICTURE

Figure 48 - Optical Photomicrographs From Three Orientations (TOP, EDGE, And END) of Springs DB-9 (Right) and DB-10 (Left) Showing the Ferrite Stringers Parallel to the Rolling Direction. Electrolytic 10% Ammonium Persulfate Etch. 500X.

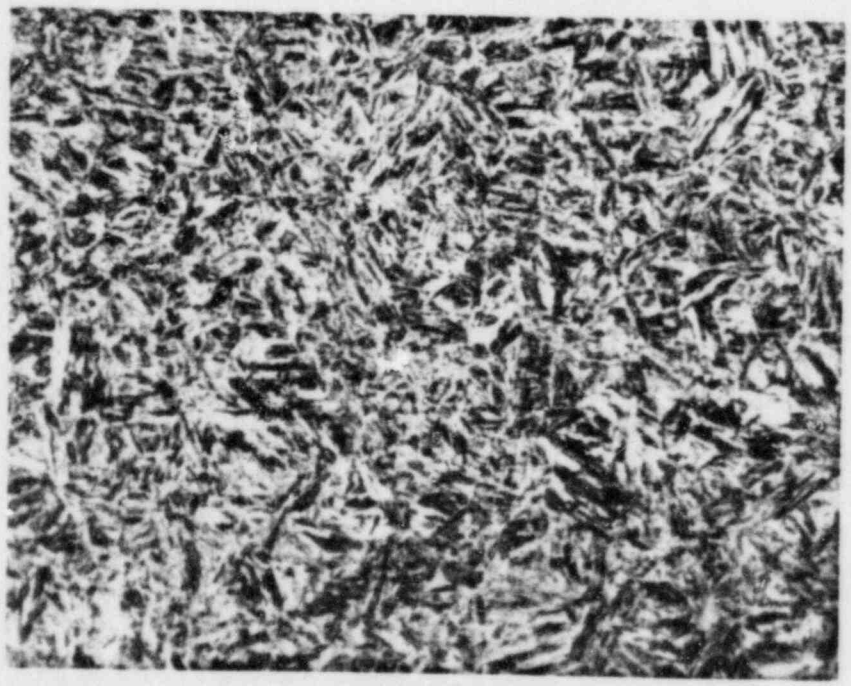

Figure 49 - Optical Photomicrograph of the Martenistic Structure in Debris Sample DB-3. Nital Etch. 1000X.

Docket No. 50-346
License No. NPF-3
Serial No. 1-525
May 15, 1985
Enclosure 2
Attachment C

CRDM LEAF SPRING DATA FOR HEAT 230232

On May 1, 1985 three leaf springs (P/N 705031-1104) were provided to the Lynchburg Research Center for additional testing. These leaf springs (S/Ns 1152, 1379 & 1453) were procured by Diamond Power in May, 1974. The material heat for the subject leaf springs is 230232. Attached are copies of the following records:

- Viking Steel Co. Material Certification (corrected) dated December 5, 1974.
- DPSC furnace chart for the subject heat dated October 7, 1974.
- DPSC Met. Lab Report No. 664 dated November 21, 1974.

VIKING STEEL COMPANY

WHERE DEPENDABILITY IS THE FIRST QUALITY OF THE MATERIAL

16700 ST CLAIR AVENUE
CLEVELAND OHIO 44110
Phone [illegible]

TO HPL McNeary Ohio
23401 Solon Rd
Solon Ohio 44133

DATE 12 - - 74

TYPE 17-7 CHT
H 2 D Fin

YOUR ORDER NO 87734
OUR SALE NO 22750

Corrected
Certification

CERTIFIED CHEMICAL · PHYSICAL ANALYSIS

		962 x 36 x 120
		72*
Heat Number		#230232
Carbon	(C)	.073 ✓
Manganese	(Mn)	.62 ✓
Phosphorus	(P)	.019 ✓
Sulfur	(S)	.018 ✓
Silicon	(Si)	.40 ✓
Chrome	(Cr)	17.00 ✓
Nickel	(Ni)	7.12 ✓
Molybdenum	(Mo)	.10
Columbium	(Cb)	
Tantalum	(Ta)	
Copper	(Cu)	.16
Cobalt	(Co)	.11
Titanium	(Ti)	
Aluminum	(Al)	1.22 ✓
Tin	(Sn)	
Iron	(Fe)	
Selenium	(Se)	
Tungsten	(W)	
Tensile Strength—PSI		127723 ✓
Yield Strength—PSI		42102 ✓
Elongation		42.5% ✓
Red. Area		
Hardness		RB 85 ✓
Hardenability		
Bend Test		
Special Test		

UCL IC [illegible]
RQC

DEC 9 1974

Sworn to and subscribed before me
this [illegible] day of December 19[illegible]

VIKING STEEL COMPANY

[illegible]

BY [illegible]

[illegible] 5, 19[illegible]

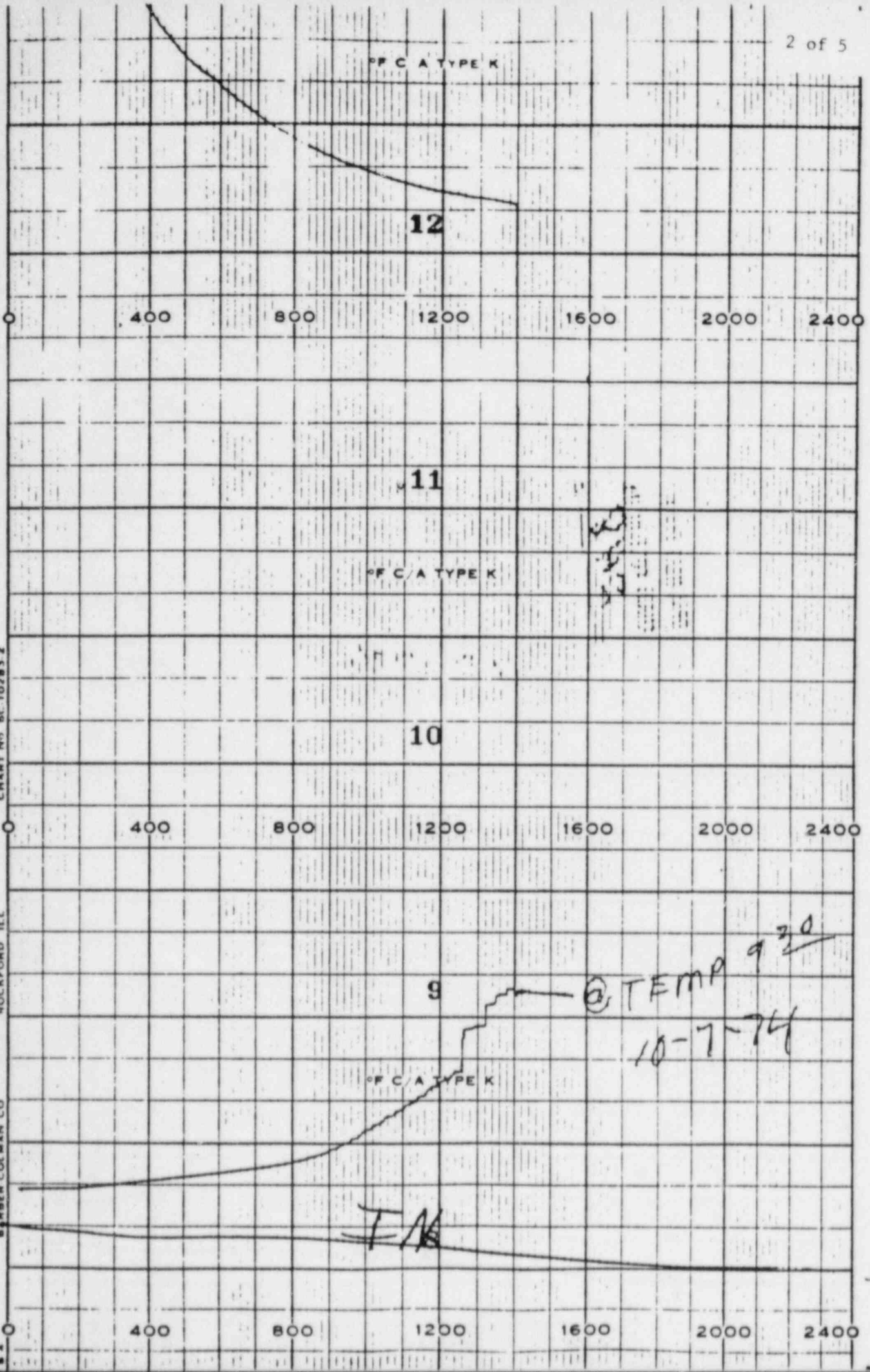

CHART NO SC 10283.2

ROCKFORD ILL

BARBER COLMAN CO

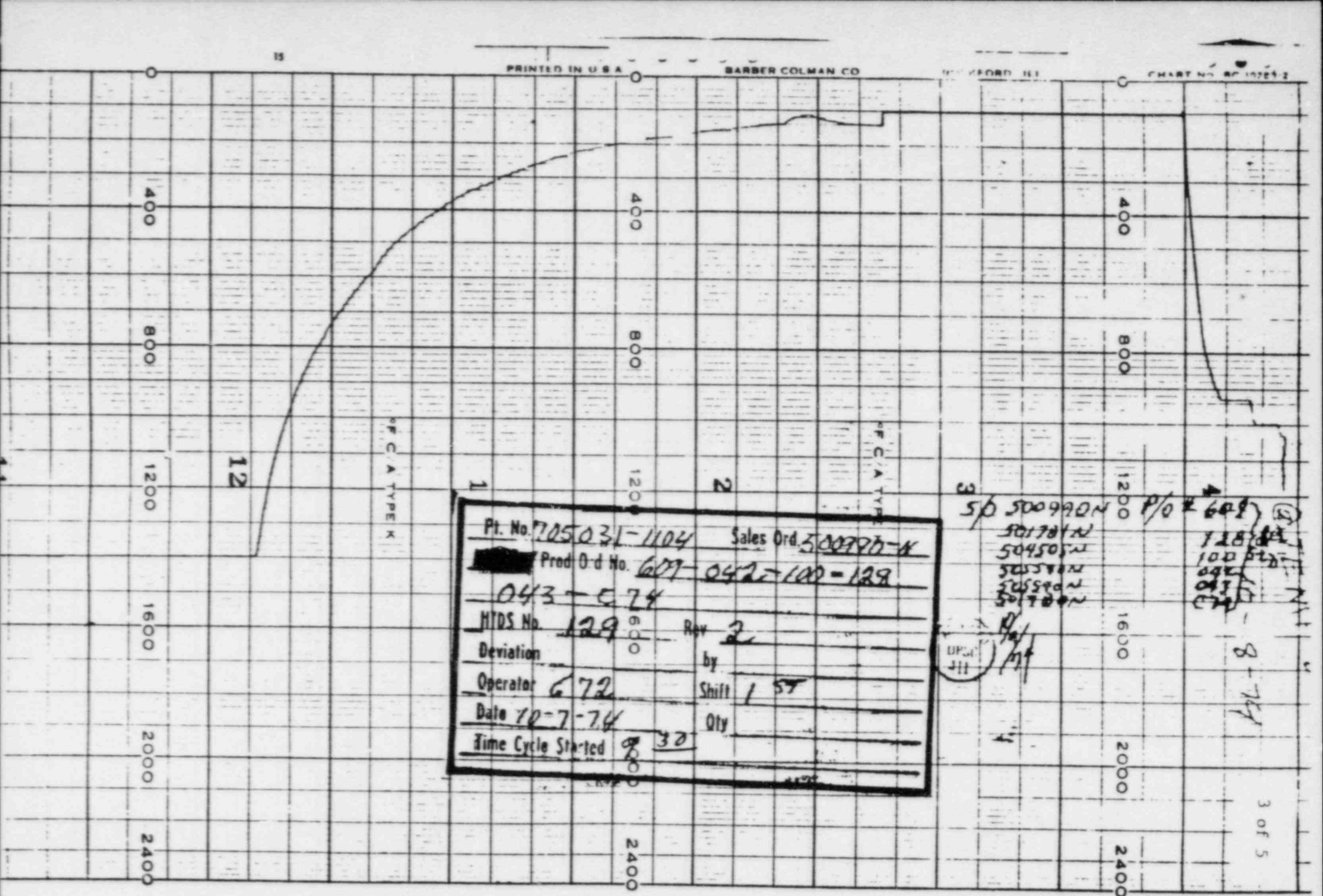
PRINTED IN U.S.A.
BARBER COLMAN CO
CHART NO. BC 10769-2
400
800
1200
1600
2000
2400
12
1
2
3
4
°F C A TYPE K
Pt. No. 705031-1104
Sales Ord. 500990-N
Prod Ord No. 607-042-100-129
043-674
MTDS No. 129
Rev 2
Deviation
by
Operator 672
Shift 1 ST
Date 10-7-74
Qty
Time Cycle Started 8:30
5/0 500990N P/O # 607
8-74
3 of 5

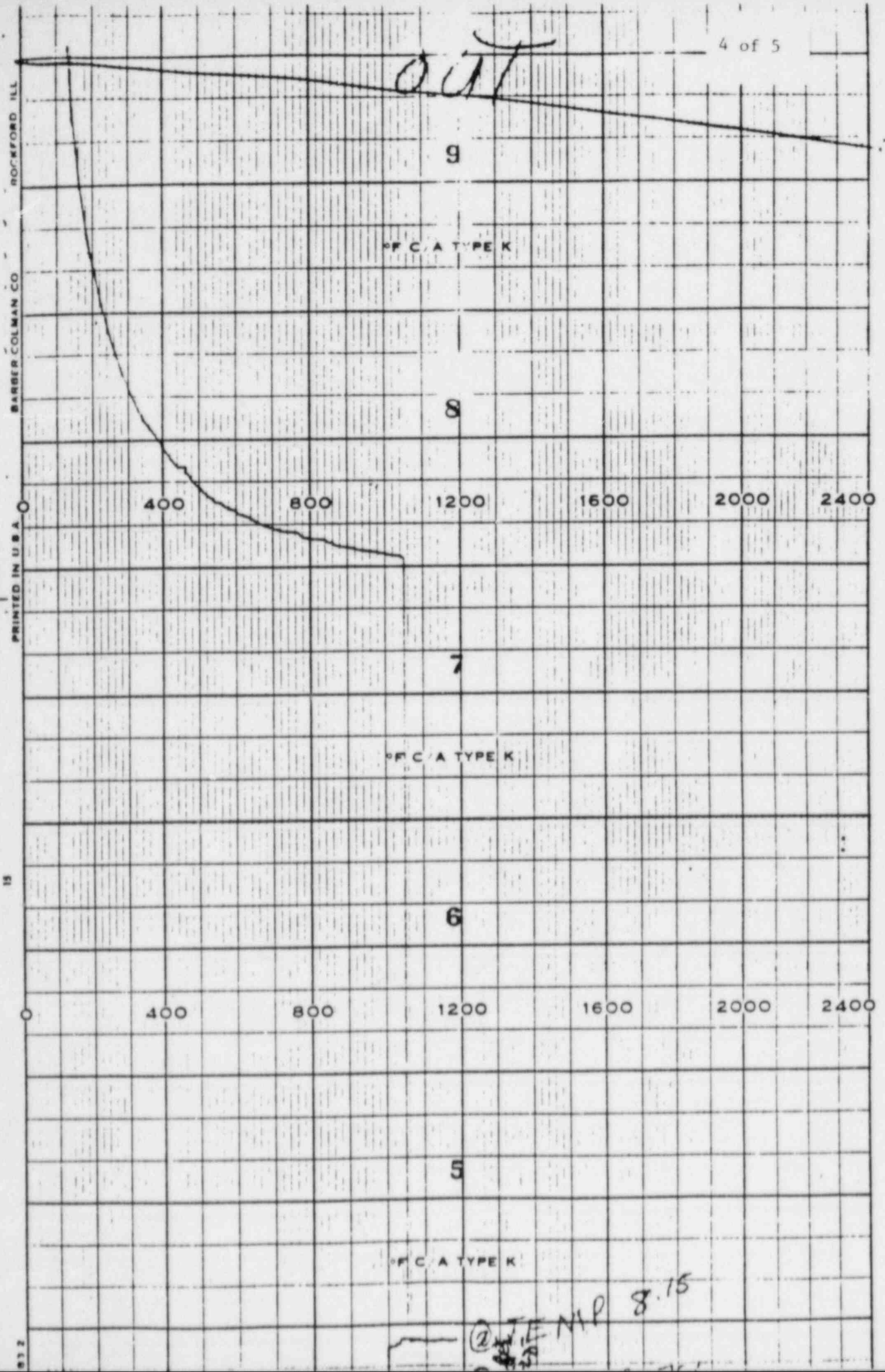
OUT
9
°F C A TYPE K
8
400
800
1200
1600
2000
2400
7
°F C A TYPE K
6
400
800
1200
1600
2000
2400
5
°F C A TYPE K
BARBER COLMAN CO ROCKFORD ILL
PRINTED IN U S A

R. D. KOESTER
H. LYNCH
W. KLINGLER

R. BLOCK, MET. LAB.

METALLURGICAL LABORATORY REPORT
MECHANICAL TESTS

DATE 11-21-74 CONTRACT NO. SC1780-N REPORT NO. 664

PART NO. 705031-1104 LEAF SPRING SERIAL NO. 1101 – 1160 P.O. NO. C-74

MATERIAL: TYPE 17-7 PH SPECIFICATION AMS 5528 HEAT NO. 230232 (P.O. 4103 C)

CONDITION H-1050 PER HT-1C (HTOS 129 ISSUE #2)

TENSILE TEST: PROCEDURE ASTM A370 TYPE SUB SIZE SHEET MD-0034-P

TEST DATA	Pc #3	Pc #4	~~Pc #5~~	REQUIRED
ORIGINAL SIZE	.261 x .059	.252 x .059		.250 ±.002 x t
ORIGINAL AREA	.0154	.0149		
ORIGINAL GAGE LENGTH	1.000	1.000		1.000 ±.003
LOAD, LBS. (DIAL)	2945	3045		
STRENGTH, PSI	191,234	204,362		180,000
YIELD, LBS.	2700	2610		
YIELD, PSI	175,325	175168		150,000
FINAL DIA.	N/A	N/A		
FINAL AREA	N/A	N/A		
REDUCTION OF AREA, %	N/A	N/A		N/A
FINAL GAGE LENGTH	1.055 *	1.09		
ELONGATION, %	5.5 *	9.0		6

REMARKS ON RESULTS SEE C.P.I. BELOW **

~~IMPACT TEST: PROCEDURE~~ ~~TYPE~~

~~TEST DATA~~	~~Pc #1~~	~~Pc #2~~	~~Pc #3~~	~~REQUIRED~~
~~TEMPERATURE, °F.~~				
~~FT. LBS.~~				
~~LATERAL EXPANSION, IN.~~				
~~DUCTILE FRACTURE, %~~				
~~HARDNESS CHECK, R_C~~				

~~REMARKS ON RESULTS~~

OTHER PERTINENT INFORMATION

* SPECIMEN BROKE IN GA. ; MARK AREA; THEREFORE ELONGATION AND Pc. #3 IS NOT REPRESENTATIVE. RETEST SPECIMEN IS Pc. #4

** THE ABOVE RESULTS INDICATE THAT THE MECHANICAL PROPERTIES ARE ACCEPTABLE TO THE HT-1C REQUIREMENTS. HOWEVER, HT-1C REQUIRES THAT ENOUGH MATERIAL BE INCLUDED WITH EACH HEAT TREAT LOT TO MAKE A STANDARD MECH. TEST SPECIMEN (NORMALLY 2" GAGE LENGTH). PER W.O. KLINGLER, THE VENDOR DID NOT HAVE ANY EXTRA MATERIAL; THEREFORE ACTUAL PARTS WERE USED FOR THIS TENSILE TEST. THIS TECHNIQUE DOES HAVE THE ADVANTAGE OF ASSURING THAT THE SAME MATERIAL IS USED.
REFERENCE: LAB REPORT #40 & #42

TEST MADE BY Hilary Carpenter DATE 11-21-74

MET ENGINEER R. E. Koester DATE 11-21-74

DF-5778 A

Docket No. 50-346
License No. NPF-3
Serial No. 1-525
May 15, 1985
Enclosure 3

DAVIS-BESSE NUCLEAR POWER STATION UNIT NO. 1
RESULTS OF RCS CHEMICAL ANALYSIS

Compound	Concentration (ppb)	Limit of Detectability (ppb)
Sulfate (SO_4)	32	0.5
Chloride (Cl)	16	0.05
Phosphate (PO_4)	11	0.5
Nitrate (NO_3)	16	0.5

Testing was performed by NWT Corporation based in San Jose, California. The RCS sample was obtained from Davis-Besse with the reactor at 90% power on May 2, 1985.

LEAF SPRING FAILURE MECHANISM VALIDATION PROGRAM

The following is a description of the proposed program to be performed to validate the leaf spring failure mechanism. The work performed under this program will establish a data base from existing inspections, laboratory examinations and analyses. Added to this data base will be information from a literature search and from the collection of data on the material processing and fabrication procedures used in the manufacture of the Davis-Besse leaf springs. A search will also be made to identify the heat numbers of 17-7 PH material from which CRDM leaf springs have been made and to locate their Certified Material Test Reports.

Additionally, non-destructive examination results of leaf springs removed from other operating plants during recent inspections will be included in the data base.

After an evaluation of this data base, a decision will be made whether to recommend further testing. Upon decision relative to test program recommendations, a final report will be prepared containing the data base information necessary to provide further validation of the identified failure mechanism. Included in the report will be a description of a recommended test program, if needed, to augment the data base sufficiently to support the objective.

Attached is a flow chart showing the steps in the proposed program to develop testing recommendations and issue a final report, and a chart describing the program objective and logic to reach that objective.

cj b/41

CRDM LEAF SPRING FAILURE MODE VALIDATION PLAN

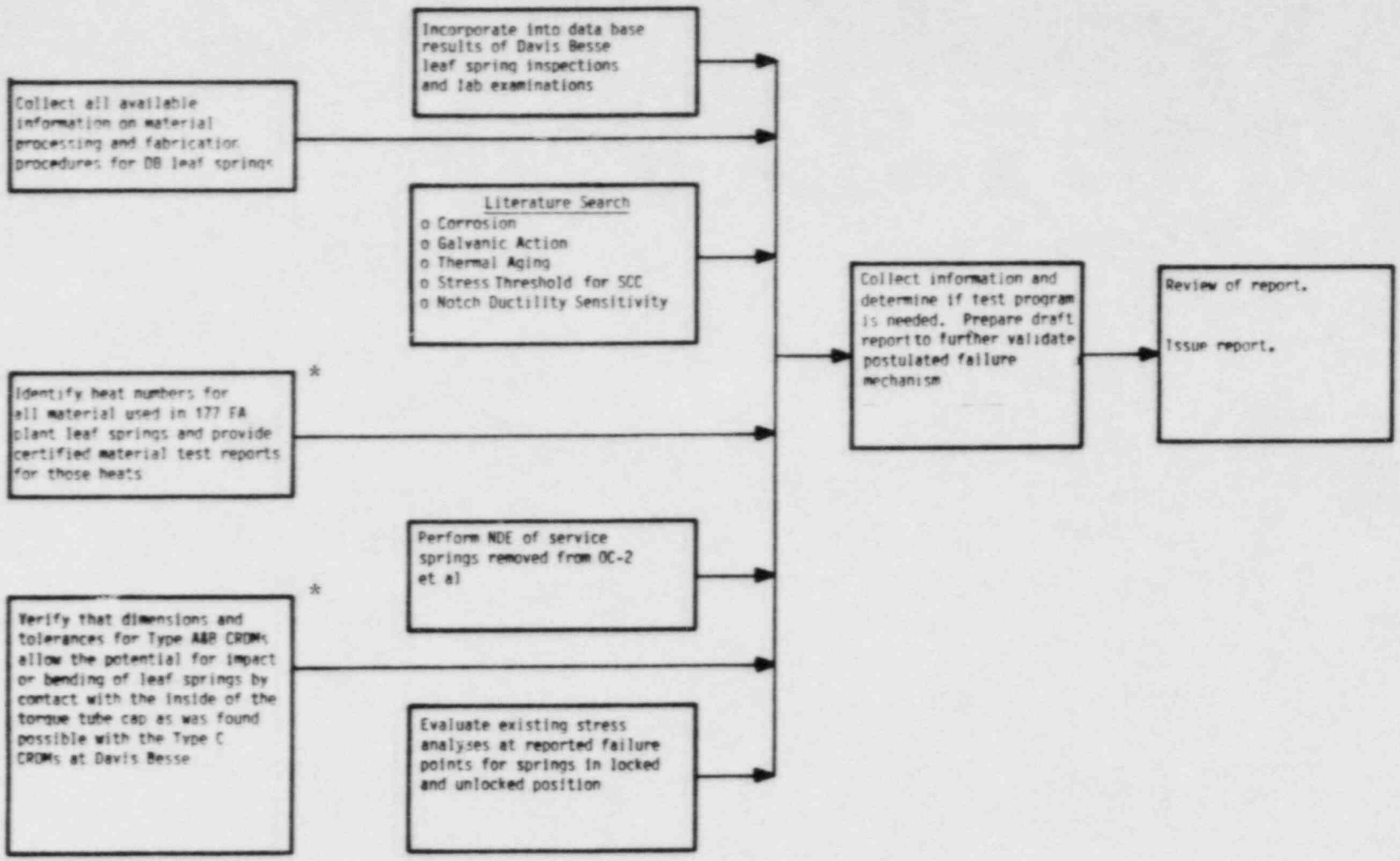

* Proposed as additions for B&W Owners Group program.

PROGRAM LOGIC

POSTULATED FAILURE MECHANISM	Demonstrated By:
Intergranular failure due to impact or bending by contact with inside of torque tube cap.	Laboratory examinations of Davis Besse leaf springs. Tolerance studies. Loading analysis. Three point bending test in hot water.

Program Objective:

Validate postulated failure mechanism by showing that failure is not the result of:

Potential Failure Mechanism	To Rule Out This Mechanism Show	Demonstrated By:
Galvanic Action and General Corrosion	CRDM leaf spring corrosion rate in expected environment is low.	Data from literature search supported by accelerated corrosion testing, if necessary
Thermal Aging	Material and physical properties of 17-7PH material are stable at CRDM leaf spring service temperatures.	Data from literature search supported by accelerated creep testing, if necessary.
Stress Corrosion Cracking	Show actual stress is well below where failure would be expected, or establish a stress threshold for SCC. Contaminants that lead to SCC not found on failed springs.	Data from literature search. Compare data from Boeing and others obtained from literature to calculated stress levels in leaf springs in locked & unlocked condition. Data from microprobe analysis. Laboratory examinations of leaf springs from Davis Besse, Oconee-2 et al.
H_2 Embrittlement	Show that a significant loss of ductility has not occurred in service samples.	Data from literature Bench mark by testing of ductility of service samples compared to non-service samples
Crevice Cracking	Examination of service samples does not show accelerated attack in crevice area. Contaminants not found that could lead to such attack.	Laboratory examination of Davis Besse leaf springs and service samples from Oconee-2 et al. Microprobe analysis data.